

Twisted kink crystal in the chiral Gross-Neveu model

Gökçe Başar and Gerald V. Dunne

Physics Department, University of Connecticut, Storrs, Connecticut 06269, USA

(Received 16 June 2008; published 11 September 2008)

We present the detailed properties of a self-consistent crystalline chiral condensate in the massless chiral Gross-Neveu model. We show that a suitable ansatz for the Gorkov resolvent reduces the functional gap equation, for the inhomogeneous condensate, to a nonlinear Schrödinger equation, which is exactly soluble. The general crystalline solution includes as special cases all previously known real and complex condensate solutions to the gap equation. Furthermore, the associated Bogoliubov-de Gennes equation is also soluble with this inhomogeneous chiral condensate, and the exact spectral properties are derived. We find an all-orders expansion of the Ginzburg-Landau effective Lagrangian and show how the gap equation is solved order by order.

DOI: [10.1103/PhysRevD.78.065022](https://doi.org/10.1103/PhysRevD.78.065022)

PACS numbers: 11.10.Kk, 11.30.Rd, 71.10.Pm

I. INTRODUCTION

In a recent paper [1], the authors found a new self-consistent *crystalline* condensate solution to the gap equation of the massless chiral Gross-Neveu model [2]. For this complex chiral condensate, the amplitude is periodic and the phase winds by a certain angle over each period. Our approach is based on the observation that a carefully motivated ansatz for the associated Gorkov resolvent reduces the gap equation to a simple ordinary differential equation, an explicitly soluble form of the nonlinear Schrödinger equation (NLSE). In general, the gap equation for an *inhomogeneous* condensate is a highly nontrivial functional differential equation, so the reduction to the NLSE represents a significant simplification. This resolvent approach is complementary to the inverse scattering approach [3,4], which also dramatically simplifies the gap equation, but which was not developed for periodic inhomogeneities. Our resolvent method is based on an extension, to complex and periodic condensates, of the work of Feinberg and Zee [5,6]. The general solution to the nonlinear Schrödinger equation contains all previously known self-consistent condensates of the massless Gross-Neveu models [both chiral and nonchiral] as special cases: the single real kink [3], the single complex kink [4], the real kink crystal [7], and the complex chiral spiral [8], and also yields a new complex kink crystal [1]. In the language of condensed matter physics, this crystalline condensate is a new solution of the Eilenberger equation (for the Gorkov resolvent) [9], and we also present here the complete exact solution of the associated Bogoliubov-de Gennes (BdG) [10] equation $H\psi = E\psi$ for this system. The Eilenberger and Bogoliubov-de Gennes equations are fundamental elements of the treatment of a wide class of interacting fermion systems, which are important in many branches of physics, ranging from particle physics to solid state and atomic physics [11–14]. Important paradigms include the Peierls-Frohlich model of conduction [15], the Gorkov-Bogoliubov-de Gennes approach to superconductivity

[10], and the Nambu–Jona-Lasinio (NJL) model of symmetry breaking in particle physics [16]. Here we study a 1 + 1-dimensional version of the NJL model, the NJL_2 model (also known as the *chiral* Gross-Neveu model, χGN_2). This model has been widely studied as it exhibits asymptotic freedom, dynamical mass generation, and chiral symmetry breaking [2–5].

Our primary physical motivation for studying the gap equation of the massless chiral Gross-Neveu model, the NJL_2 model, is to understand the (T, μ) phase diagram of this system. Somewhat surprisingly, the phase diagram of this system is not yet fully understood. A gap equation analysis based on a homogeneous condensate suggests its phase diagram is the same as its discrete-chiral cousin, the original Gross-Neveu (GN_2) model [2], while more recent work finds an inhomogeneous Larkin-Ovchinnikov-Fulde-Ferrell (LOFF [17]) helical complex condensate (“chiral spiral”) below a critical temperature [8]. In [1], a Ginzburg-Landau approach was used to show that in a region of the phase diagram the free energy is lower for a complex kink crystal, compared to a uniform condensate or a chiral spiral condensate. In this paper we present the details of the complex crystalline condensate of the NJL_2 system, and also the *exact* spectral properties of fermions in the presence of such a crystalline condensate. This information will subsequently be used to study the free energy exactly, without resorting to the Ginzburg-Landau approximation.

This state of affairs should be compared and contrasted with the case of the original Gross-Neveu model [2], to which we refer as the GN_2 model, which has a *discrete* chiral symmetry rather than the continuous chiral symmetry of the NJL_2 model. In the GN_2 model, the phase diagram has only relatively recently been solved in the particle physics literature, analytically and exactly by a Hartree-Fock analysis [7], and numerically on the lattice [18]. There is a crystalline phase at low temperature and high density, and this phase is characterized by a periodically inhomogeneous (real) condensate that solves exactly

the gap equation. This phase is not seen in the old phase diagram which was based on a uniform condensate [19,20]. Interestingly, some hints of a problem with the homogeneous condensate assumption were found already in an early lattice study [21]. This discrete-chiral GN_2 model (with vanishing bare fermion mass) turns out to be mathematically equivalent to several models in condensed matter physics [7]: the real periodic condensate may be identified with a polaron crystal in conducting polymers [11,22,23], with a periodic pair potential in quasi-1D superconductors [24–26], and with the real order parameter for superconductors in a ferromagnetic field [27]. The Gross-Neveu models also serve as paradigms of the phenomenon of fermion number fractionalization [28–31].

Here, we consider the massless chiral Gross-Neveu, or NJL_2 , model in $1 + 1$ dimensions with the Lagrangian [2–4]

$$\mathcal{L} = \bar{\psi}i\not{\partial}\psi + \frac{g^2}{2}[(\bar{\psi}\psi)^2 + (\bar{\psi}i\gamma^5\psi)^2]. \quad (1.1)$$

This system has a continuous chiral symmetry under $\psi \rightarrow e^{i\gamma^5\alpha}\psi$. We have suppressed summation over N flavors, which makes the semiclassical gap equation analysis exact in the $N \rightarrow \infty$ limit, a limit in which we can consistently discuss chiral symmetry breaking in 2D [32,33]. The original Gross-Neveu model, the GN_2 model [2], without the pseudoscalar interaction term $(\bar{\psi}i\gamma^5\psi)^2$, has a discrete chiral symmetry $\psi \rightarrow \gamma^5\psi$.

There are two equivalent ways to find self-consistent static condensates. First, we introduce bosonic scalar and pseudoscalar condensate fields, σ and π , which we combine into a complex condensate field, defined either through its real and imaginary parts, or via its amplitude and phase:

$$\Delta \equiv \sigma - i\pi \equiv Me^{i\chi}. \quad (1.2)$$

Integrating out the fermion fields we obtain an effective action for the condensate Δ as

$$S_{\text{eff}} = -\frac{1}{2g^2} \int |\Delta|^2 - iN \text{Indet} \left[i\not{\partial} - \frac{1}{2}(1 - \gamma^5)\Delta - \frac{1}{2}(1 + \gamma^5)\Delta^* \right]. \quad (1.3)$$

The corresponding (complex) gap equation is

$$\Delta(x) = -2iNg^2 \frac{\delta}{\delta\Delta(x)^*} \text{Indet} \left[i\not{\partial} - \frac{1}{2}(1 - \gamma^5)\Delta(x) - \frac{1}{2}(1 + \gamma^5)\Delta^*(x) \right]. \quad (1.4)$$

If the condensate is constant, as is usually assumed, it is straightforward to evaluate the determinant and solve the gap equation [13,19,20]. When the condensate is inhomogeneous, this is a much more difficult problem. Dashen, Hasslacher, and Neveu [3] used inverse scattering to find

kinklike static but spatially inhomogeneous condensates for the gap equation of the GN_2 model (where there is no pseudoscalar condensate, so Δ is real). Shei [4] extended this inverse scattering analysis to the chiral Gross-Neveu model, the NJL_2 model, and found a spatially inhomogeneous complex kink. A new approach to the inhomogeneous gap equation, based on the resolvent, was developed by Feinberg and Zee [5] and applied to the kink solutions of both the GN_2 and NJL_2 models. For the GN_2 model, Thies used a Hartree-Fock approach to find a periodic extension of the real kink solution, motivated by analogous inhomogeneous condensates in condensed matter systems [7]. In [1], the present authors showed that the complex gap equation (1.4) can be reduced in an elementary manner to a soluble form of the nonlinear Schrödinger equation. The general solution contains all previously known inhomogeneous condensates (real and complex), and yields a new crystalline extension of Shei's complex kink.

A second approach to finding a self-consistent condensate is to solve the relativistic Hartree-Fock problem $H\psi = E\psi$, with the single-particle Hamiltonian

$$H = -i\gamma^5 \frac{d}{dx} + \gamma^0 \left[\frac{1}{2}(1 - \gamma^5)\Delta(x) + \frac{1}{2}(1 + \gamma^5)\Delta^*(x) \right] \quad (1.5)$$

and subject to the consistency condition

$$\langle \bar{\psi}\psi \rangle - i\langle \bar{\psi}i\gamma^5\psi \rangle = -\Delta/g^2. \quad (1.6)$$

We choose Dirac matrices $\gamma^0 = \sigma_1$, $\gamma^1 = -i\sigma_2$, $\gamma^5 = \sigma_3$, to emphasize the natural complex condensate combination in (1.2). Then the single-particle Hamiltonian is

$$H = \begin{pmatrix} -i\frac{d}{dx} & \Delta(x) \\ \Delta^*(x) & i\frac{d}{dx} \end{pmatrix}. \quad (1.7)$$

This Hamiltonian is also known as the BdG Hamiltonian, and we will refer to the associated spectral equation

$$H\psi = E\psi \quad (1.8)$$

as the BdG equation.

In Sec. II we review the reduction of the functional gap equation to the NLSE, and in Secs. III and IV we present the real and complex condensates obtained from solving the NLSE. In Sec. V we show that the associated Bogoliubov-de Gennes equation can also be solved exactly, and we derive the exact single-particle spectrum and density of states. In Sec. VI we verify the consistency of our solutions by solving the gap equation in the Hartree-Fock approach. An all-orders Ginzburg-Landau expansion of the free energy is presented in Sec. VII, and we show that the inhomogeneous gap equation is satisfied order by order in an interesting and nontrivial way. In a concluding section we review our results and discuss implications for the phase diagram of the chiral Gross-Neveu model.

II. REDUCTION OF FUNCTIONAL GAP EQUATION TO NONLINEAR SCHRÖDINGER EQUATION

In this section we review the reduction [1] of the functional gap equation (1.4) to the nonlinear Schrödinger equation. The key quantity in our approach is the coincident limit of Gorkov Green's function, or the “diagonal resolvent”:

$$R(x; E) \equiv \langle x | \frac{1}{H - E} | x \rangle. \quad (2.1)$$

The resolvent (2.1) is clearly a 2×2 matrix. For a static (but possibly spatially inhomogeneous) condensate, all spectral information is encoded in the resolvent. Indeed, the spectral function characterizing the single-particle spectrum of fermions in the presence of the condensate $\Delta(x)$ is

$$\rho(E) = \frac{1}{\pi} \text{Im Tr}_{D,x} [R(x; E + i\epsilon)], \quad (2.2)$$

where the trace is a Dirac trace as well as a spatial trace.

Our first, very simple, observation is that the form of the BdG equation (1.8) places very strong constraints on the possible form of $R(x; E)$. For any static condensate $\Delta(x)$, $R(x; E)$ must satisfy the following algebraic conditions [these are explained in more detail in Appendix A]:

$$R = R^\dagger, \quad (2.3)$$

$$\text{tr}_D(R(x; E)\sigma_3) = 0, \quad (2.4)$$

$$\det R(x; E) = -\frac{1}{4}. \quad (2.5)$$

Furthermore, $R(x; E)$ must satisfy the first-order differential equation

$$\frac{\partial}{\partial x} R(x; E)\sigma_3 = i \left[\begin{pmatrix} E & -\Delta(x) \\ \Delta^*(x) & -E \end{pmatrix}, R(x; E)\sigma_3 \right]. \quad (2.6)$$

In superconductivity, (2.6) is known as the Eilenberger equation [9,34], and in mathematical physics as the Dikii equation [35]. These conditions (2.3), (2.4), and (2.5), and the Eilenberger equation (2.6), all follow from the simple fact [34–36] that for the one-dimensional BdG equation, which involves derivatives with respect to the single variable x , the Green's function can be expressed as a product of two independent solutions to (1.8):

$$R(x; E) = \frac{1}{2iW} (\psi_1 \psi_2^T + \psi_2 \psi_1^T) \sigma_1 \quad (2.7)$$

where W is the Wronskian of two independent solutions $\psi_{1,2}$: $W = i\psi_1^T \sigma_2 \psi_2$.

The next step is to note that the gap equation provides further information about the possible form of the resolvent, and this is enough to motivate a specific ansatz form [1]. There are two ways of viewing the gap equation (1.4)

in terms of the resolvent. First, for a static condensate we can write the log det term in the effective action (1.3) as minus the grand canonical potential, in terms of the single-particle spectral function $\rho(E)$:

$$-\frac{1}{\beta} \int_{-\infty}^{\infty} dE \rho(E) \ln(1 + e^{-\beta(E-\mu)}). \quad (2.8)$$

All dependence on $\Delta(x)$ resides in the spectral function $\rho(E)$, via (2.2). Therefore, inserting this into the gap equation (1.4), this relates $\Delta(x)$ to the *diagonal* entries of $R(x; E)$. Further, as a consequence of the condition (2.4), these diagonal entries are equal. So, the simplest natural solution to the gap equation is for the diagonal entries of $R(x; E)$ to be linear in $|\Delta(x)|^2$. A second way to view the gap equation is to evaluate the functional derivative in (1.4), which for a static condensate leads to

$$\Delta(x) = -iNg^2 \text{tr}_{D,E} [\gamma^0 (\mathbf{1} + \gamma^5) R(x; E)]. \quad (2.9)$$

The Dirac trace then relates the *off-diagonal* entries of $R(x; E)$ to $\Delta(x)$. Since R is Hermitian, these off-diagonal entries are complex conjugates of one another.

Summarizing, $R(x; E)$ must be a Hermitian 2×2 matrix with equal diagonal entries, such that (after the spatial and energy trace) the variation of the diagonal terms is proportional to $\Delta(x)$, and with off-diagonal terms linear in $\Delta(x)$, after the energy trace. This suggests taking the resolvent to be of the form

$$R(x; E) = \mathcal{N}(E) \begin{pmatrix} a(E) + |\Delta(x)|^2 & b(E)\Delta(x) \\ b(E)\Delta^*(x) & a(E) + |\Delta(x)|^2 \end{pmatrix} \quad (2.10)$$

where $a(E)$, $b(E)$, and $\mathcal{N}(E)$ are functions of E , independent of x , and are to be determined. However, this ansatz cannot describe inhomogeneous condensates because the only solution of this form consistent with (2.5) is a condensate with constant magnitude, independent of x . Indeed, taking Δ to be constant (and by a global chiral rotation, real), $\Delta = M$, the solution to (2.3), (2.4), (2.5), and (2.6) is simply

$$R(x; E) = \frac{1}{2\sqrt{M^2 - E^2}} \begin{pmatrix} E & M \\ M & E \end{pmatrix}, \quad (2.11)$$

as is familiar. This example also illustrates that the Hermiticity condition (2.3) must of course be interpreted with the appropriate $i\epsilon$ prescription for the energy.

To find inhomogeneous condensates, we suggested in [1] to extend the ansatz (2.10) to include a first derivative term in the off-diagonal entries:

$$R(x; E) = \mathcal{N}(E) \times \begin{pmatrix} a(E) + |\Delta(x)|^2 & b(E)\Delta(x) - i\Delta'(x) \\ b(E)\Delta^*(x) + i\Delta'^*(x) & a(E) + |\Delta(x)|^2 \end{pmatrix}. \quad (2.12)$$

This is the simplest extension of (2.10) that is consistent

with the various algebraic constraints and with the Eilenberger equation (2.6). Indeed, substituting the ansatz (2.12) into the Eilenberger equation (2.6), we see that the diagonal entry of this equation is identically satisfied, while the off-diagonal entry implies that $\Delta(x)$ must satisfy the following NLSE [and its complex conjugate]:

$$\Delta'' - 2|\Delta|^2\Delta + i(b - 2E)\Delta' - 2(a - Eb)\Delta = 0. \quad (2.13)$$

Two comments are in order. First, it is not immediately obvious that $R(x; E)$ in (2.12) can satisfy the normalization condition (2.5) for an inhomogeneous condensate, since

$$\det R(x; E) = \mathcal{N}^2\{|\Delta|^4 - |\Delta'|^2 + (2a - b^2)|\Delta|^2 + ib(\Delta'\Delta^* - \Delta\Delta'^*) + a^2\}. \quad (2.14)$$

Remarkably, the NLSE (2.13) implies that $(\det R(x; E))$ is constant:

$$\begin{aligned} \frac{d}{dx} \left(\frac{\det R(x; E)}{\mathcal{N}^2} \right) &= (2|\Delta|^2 + 2a - b^2)(|\Delta|^2)' \\ &\quad - (\Delta''\Delta'^* + \Delta'\Delta''^*) \\ &\quad + ib(\Delta''\Delta^* - \Delta^*\Delta'') = 0 \end{aligned} \quad (2.15)$$

where we have used the fact that the NLSE (2.13) implies that $(\Delta''\Delta'^* + \Delta'\Delta''^*) = (2|\Delta|^2 + 2a - 2Eb)(|\Delta|^2)'$, and that $(\Delta''\Delta^* - \Delta^*\Delta'') = -i(b - 2E)(|\Delta|^2)'$. Since $\det R(x; E)$ is constant, the normalization in (2.5) can be achieved by a suitable choice of $\mathcal{N}(E)$. Second, while the ansatz (2.12) automatically satisfies the x dependence of the gap equation in its form coming from (2.8) (because the trace of R is, by construction, linear in $|\Delta|^2$), it does not satisfy the other form of the gap equation (2.9), until the energy trace is performed. This is because of the $\Delta'(x)$ terms in the off-diagonal. In Sec. VI we show that this form of the gap equation is indeed satisfied because the coefficient of the $\Delta'(x)$ term vanishes due to the energy trace.

Thus, we have reduced the very difficult problem of solving the functional gap equation (1.4) for a self-consistent condensate $\Delta(x)$ to the much simpler problem of solving the NLSE for $\Delta(x)$. In fact, the NLSE (2.13) is explicitly soluble, as is discussed in the following sections, in which we describe first the real solutions (relevant for the GN₂ model), and then the complex solutions (relevant for the NJL₂ model).

III. REAL SOLUTIONS OF THE NLSE

In this section we recall the previously known *real* solutions to the gap equation, and show how they fit in with the NLSE (2.13) and the resolvent form in (2.12).

A. Homogeneous condensate

If the condensate is constant, then by a global chiral rotation it can be taken to be real:

$$\Delta(x) = m. \quad (3.1)$$

This clearly satisfies the NLSE (2.13), and we find

$$a(E) = 2E^2 - m^2, \quad b(E) = 2E, \quad \mathcal{N}(E) = \frac{1}{4} \frac{1}{E\sqrt{m^2 - E^2}}. \quad (3.2)$$

The spectrum of the associated BdG equation (1.8) is that of a free fermion with mass m , with positive and negative energy continua starting at $E = \pm m$, the mass scale being set by the amplitude of the condensate.

B. Single real kink condensate

A well-known nontrivial solution to the gap equation is the single (real) kink [3]:

$$\Delta(x) = m \tanh(mx). \quad (3.3)$$

This satisfies the NLSE

$$\Delta'' - 2\Delta^3 + 2m^2\Delta = 0, \quad (3.4)$$

and so we deduce the exact diagonal resolvent to be of the form (2.12) with

$$a(E) = 2E^2 - m^2, \quad b(E) = 2E, \quad \mathcal{N}(E) = \frac{1}{4} \frac{1}{E\sqrt{m^2 - E^2}}. \quad (3.5)$$

The spectrum of the associated BdG equation (1.8) has positive and negative energy continua starting at $E = \pm m$, together with a single bound state located at $E = 0$, at the center of the gap. This midgap zero mode has many important consequences in a variety of branches of physics [28,30].

C. Real kink crystal condensate

A periodic array of these real kinks also provides a solution to the gap equation. This solution describes a polaron crystal in polymer physics [22,23], a periodic pair potential in inhomogeneous superconductors [24,25,27], and the crystalline phase of the Gross-Neveu model [7]. Define (the peculiar-looking scaling will become clear below)

$$\Delta(x) = \sqrt{\nu} \frac{2m}{1 + \sqrt{\nu}} \operatorname{sn} \left(\frac{2m}{1 + \sqrt{\nu}} x; \nu \right) \quad (3.6)$$

where sn is the Jacobi elliptic function [37–40] with the real elliptic parameter $0 \leq \nu \leq 1$. The sn function has a period $2\mathbf{K}(\nu)$, where $\mathbf{K}(\nu) \equiv \int_0^{\pi/2} (1 - \nu \sin^2 t)^{-1/2} dt$. When $\nu = 1$, (3.6) reduces to the single kink condensate in (3.3). The periodic condensate (3.6) satisfies the NLSE

$$\Delta'' - 2\Delta^3 + (1 + \nu) \left(\frac{2m}{1 + \sqrt{\nu}} \right)^2 \Delta = 0. \quad (3.7)$$

Thus, we deduce the exact diagonal resolvent to be of the form (2.12) with

$$a(E) = 2E^2 - 2m^2 \frac{1 + \nu}{(1 + \sqrt{\nu})^2}, \quad (3.8)$$

$$b(E) = 2E, \quad (3.9)$$

$$\mathcal{N}(E) = \frac{1}{4} \frac{1}{\sqrt{m^2 - E^2} \sqrt{E^2 - m^2 \left(\frac{1 - \sqrt{\nu}}{1 + \sqrt{\nu}}\right)^2}}. \quad (3.10)$$

This periodic condensate is plotted in Fig. 1. Note that over the period $x \in \left[-\frac{\mathbf{K}(\nu)(1 + \sqrt{\nu})}{2m}, \frac{\mathbf{K}(\nu)(1 + \sqrt{\nu})}{2m}\right]$, the condensate is shaped like a single kink. This reflects the expansion of the Jacobi sn function in terms of an array of periodically displaced tanh functions:

$$\text{sn}(x; \nu) = \frac{\pi}{2\sqrt{\nu}\mathbf{K}'} \sum_{n=-\infty}^{\infty} (-1)^n \tanh\left(\frac{\pi}{2\mathbf{K}'}(x - 2n\mathbf{K})\right) \quad (3.11)$$

where we use the standard notation $\mathbf{K}'(\nu) \equiv \mathbf{K}(1 - \nu)$. In the infinite period limit ($\nu \rightarrow 1$), the interval $\left[-\frac{\mathbf{K}(\nu)(1 + \sqrt{\nu})}{2m}, \frac{\mathbf{K}(\nu)(1 + \sqrt{\nu})}{2m}\right]$ maps to the whole real line, and $\mathbf{K}' \rightarrow \pi/2$, so the kink crystal (3.6) reduces precisely to the single kink condensate in (3.3).

It is worth noting that this periodic kink crystal (3.6) can be written in an equivalent, but different-looking, form, by use of a Landen transformation [37–40] of the Jacobi functions. That is, by rescaling the elliptic parameter ν together with the argument mx , we can write

$$\Delta(x) = m\tilde{\nu} \frac{\text{sn}(mx; \tilde{\nu})\text{cn}(mx; \tilde{\nu})}{\text{dn}(mx; \tilde{\nu})}; \quad \tilde{\nu} = \frac{4\sqrt{\nu}}{(1 + \sqrt{\nu})^2}. \quad (3.12)$$

This is the form in which this periodic kink solution is presented in the work of Thies *et al.* [7] on the crystalline phase of the Gross-Neveu model, while the form (3.6) was used in the condensed matter literature in [22–27]. The

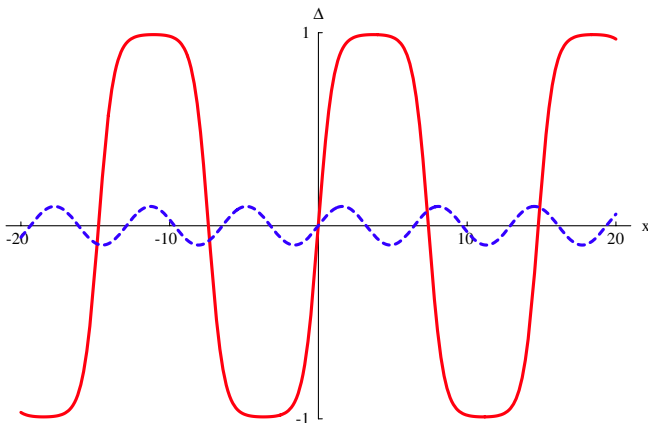


FIG. 1 (color online). The real kink crystal condensate (3.6) plotted for the elliptic parameter $\nu = 0.99$ (solid, red curve), and for $\nu = 0.1$ (dashed, blue curve). For small ν the condensate has the LOFF form of a small amplitude sinusoidal condensate, while for $\nu \rightarrow 1$ the condensate resembles an array of kinks and antikinks.

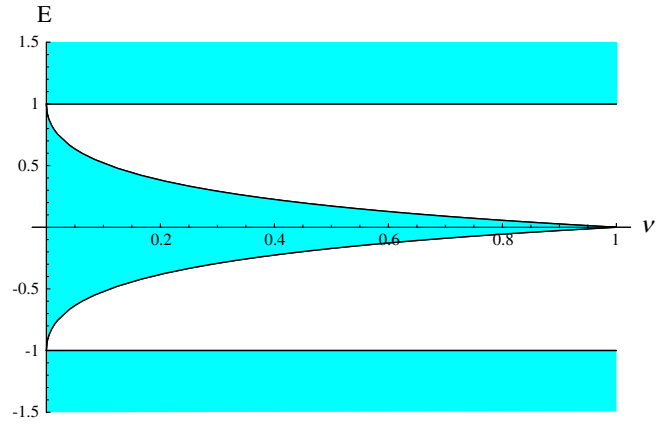


FIG. 2 (color online). The band spectrum of the real kink crystal, showing the positive and negative energy continua and the bound band, as a function of the elliptic parameter ν . The energy is given in units of the scale m . The infinite period limit is $\nu \rightarrow 1$, where the bound band shrinks to a single bound level at $E = 0$, the familiar zero mode of the kink condensate.

spectrum of the associated BdG equation (1.8) has positive and negative energy continua starting at $E = \pm m$, together with a single bound band in the middle of the gap, with band edges at $E = \pm \left(\frac{1 - \sqrt{\nu}}{1 + \sqrt{\nu}}\right)m$. This band lies symmetrically in the center of the gap. The spectrum is plotted in Fig. 2 as a function of the elliptic parameter ν . Notice that there is just one bound band in the energy gap, and when $\nu \rightarrow 1$ (the infinite period limit), the bound band at the center of the gap contracts smoothly to the single bound zero mode of the kink condensate.

IV. COMPLEX SOLUTIONS OF THE NLSE

A. Single plane-wave condensate

The simplest complex solution to the NLSE is a single plane wave:

$$\Delta = me^{iqx}. \quad (4.1)$$

This satisfies the NLSE (2.13) with

$$a(E) = 2\left(E - \frac{q}{2}\right)^2 - m^2, \quad b(E) = 2E - 2q, \quad (4.2)$$

$$\mathcal{N}(E) = \frac{1}{4} \frac{1}{(E - q/2)\sqrt{m^2 - (E - q/2)^2}}.$$

This plane-wave condensate behaves just like a constant one, but with the energy shifted by $q/2$, as can be seen by making a local chiral rotation:

$$\Delta \rightarrow e^{-iqx}\Delta, \quad \psi \rightarrow e^{-iqx/2\gamma_5}\psi. \quad (4.3)$$

It is clear from the BdG equation (1.8) that such a transformation has the effect of shifting the entire energy spectrum by $q/2$. This illustrates an important point: for complex solutions $\Delta(x)$ of the NLSE, one can always multiply by an arbitrary plane-wave phase factor e^{iqx} , and this simply corresponds to shifting the entire energy

spectrum. In general, a local chiral rotation through angle $\alpha(x)$ leads to a local chemical potential [41,42], or local electrostatic potential, $A_0(x) = \frac{1}{2}\alpha'(x)$, and therefore a local electric field $E(x) = -\frac{1}{2}\alpha''(x)$. For the single plane-wave condensate in (4.1), $\alpha(x)$ is linear in x , and so there is no associated electric field.

B. Single complex kink condensate

Shei [4] found a solution to the gap equation for the NJL₂ model, in which both the scalar and pseudoscalar condensates have a kinklike form:

$$\begin{aligned}\sigma(x) &= m[\cos^2(\theta/2) + \sin^2(\theta/2) \tanh(m \sin(\theta/2)x)], \\ \pi(x) &= -\frac{m}{2} \sin(\theta)[1 - \tanh(m \sin(\theta/2)x)]\end{aligned}\quad (4.4)$$

where $\theta \in [0, 2\pi]$ is a parameter. These kinks are plotted in Fig. 3. This complex kink (4.4) has also been extensively studied in the resolvent approach by Feinberg and Zee [5]. In our analysis it is more natural to combine these into the complex condensate $\Delta(x) = \sigma(x) - i\pi(x)$ [as in (1.2)]:

$$\Delta(x) = m \frac{\cosh(m \sin(\theta/2)x - i\theta/2)}{\cosh(m \sin(\theta/2)x)} e^{i\theta/2}. \quad (4.5)$$

This complex form is plotted in Fig. 4. This illustrates the role of the parameter $\theta \in [0, 2\pi]$ as the net rotation angle of the kink as x goes from $-\infty$ to $+\infty$:

$$\Delta(x = +\infty) = e^{-i\theta} \Delta(x = -\infty). \quad (4.6)$$

Observe that when $\theta = \pi$, the complex kink (4.5) is in fact real, and reduces to the familiar real kink solution in (3.3); this real kink changes its sign (i.e., rotates through π) in passing from $x = -\infty$ to $x = +\infty$. Another useful representation of this kink is in terms of the magnitude and phase $\Delta(x) = M(x)e^{i\chi(x)}$:

$$M^2(x) = m^2[1 - \sin^2(\theta/2)\text{sech}^2(m \sin(\theta/2)x)], \quad (4.7)$$

$$\chi(x) = \arctan\left(\frac{\sin\theta}{\cos\theta + e^{2mx \sin(\theta/2)}}\right). \quad (4.8)$$

These are plotted in Fig. 5 for three different values of the winding parameter θ . The complex kink condensate (4.5) satisfies the NLSE:

$$\Delta'' - 2|\Delta|^2\Delta - 2im \cos(\theta/2)\Delta' + 2m^2\Delta = 0. \quad (4.9)$$

From this NLSE, we deduce the exact diagonal resolvent to be of the form (2.12) with

$$\begin{aligned}a(E) &= 2E^2 - 2m \cos(\theta/2)E - m^2, \\ b(E) &= 2E - m \cos(\theta/2), \\ \mathcal{N}(E) &= \frac{1}{4(E - m \cos(\theta/2))\sqrt{m^2 - E^2}}.\end{aligned}\quad (4.10)$$

The spectrum of the associated BdG equation (1.8) has positive and negative energy continua starting at $E = \pm m$,

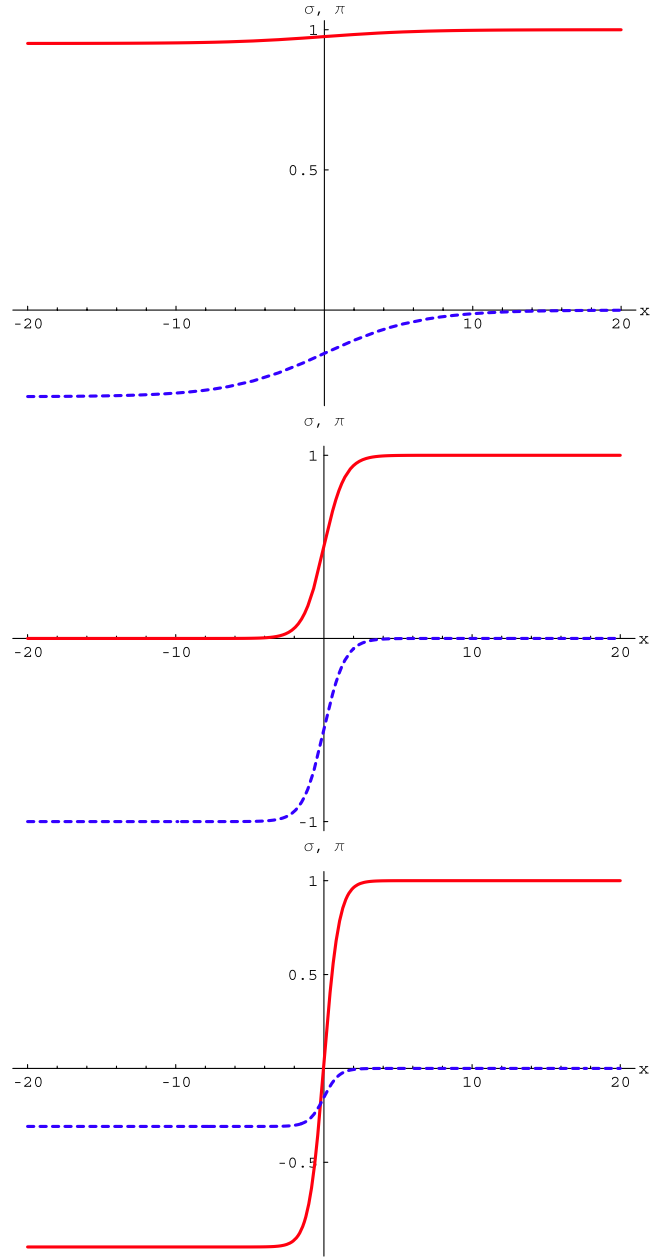


FIG. 3 (color online). Plots of the real and imaginary parts $\sigma(x)$ and $\pi(x)$ of the complex kink condensate in (4.4) for three different values of the winding parameter θ . The scalar condensate $\sigma(x)$ (solid, red curves) winds from m at $x = -\infty$ to $m \cos(\theta)$ at $x = +\infty$, while the pseudoscalar kink $\pi(x)$ (dashed, blue curves) winds from $-m \sin(\theta)$ to 0 as x ranges from $x = -\infty$ to $x = +\infty$. The plots are for $\theta = \pi/10$, $\theta = \pi/2$, and $\theta = 9\pi/10$, and σ and π are plotted in units of m .

together with a single bound state located at $E = m \cos(\theta/2)$. When $\theta = \pi$, where this complex kink reduces to the standard real kink, the bound state is once again a zero mode. But for other values of θ the single bound state lies asymmetrically inside the gap, as plotted in Fig. 6. As θ goes from 0 to 2π , one state moves from the positive to the negative energy continuum. As is clear from

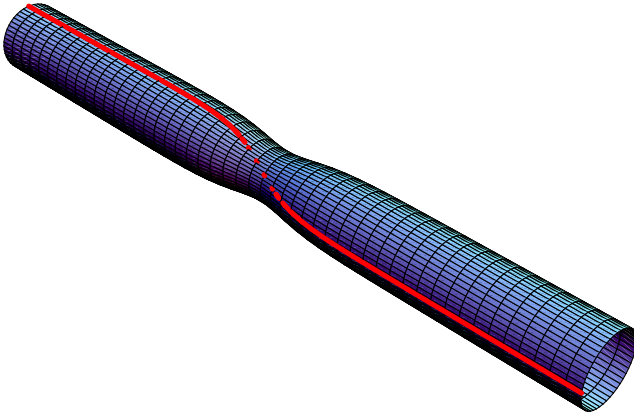


FIG. 4 (color online). Plot of the complex kink condensate (4.5), for $\theta = 3\pi/2$, illustrating how the kink winds around zero without the amplitude vanishing. The kink is the solid (red) line, and the surface is shown simply to illustrate that both the amplitude and the phase are changing.

the previous subsection, we can always multiply the complex kink solution (4.5) by a plane-wave factor e^{iqx} , which has the net effect of displacing the fermion spectrum by $q/2$, with the corresponding simple modifications to the resolvent functions $a(E)$, $b(E)$, and $\mathcal{N}(E)$ in (4.10).

At this stage we have shown that Shei's complex kink condensate (4.5) solves the NLSE, and we have found the corresponding exact diagonal resolvent (2.12) with $a(E)$, $b(E)$, and $\mathcal{N}(E)$ given in (4.10). This agrees with the spectral properties derived from inverse scattering [4]. Shei further showed [4] that this complex condensate solves the gap equation provided a further restriction is applied to the winding parameter θ . This condition states that $\theta/(2\pi)$ is equal to the filling fraction $\frac{n}{N}$ (in the large flavor limit) of the single bound state in the gap, by n flavors, with $\frac{n}{N}$ fixed as $N \rightarrow \infty$ [4,5]:

$$\frac{\theta}{2\pi} = \frac{n}{N}. \quad (4.11)$$

In Sec. VI we show that in our approach this same condition arises from demanding that the coefficient of the $\Delta'(x)$ term in (2.9) vanishes after the energy trace, a necessary requirement to satisfy the gap equation.

C. Complex kink crystal condensate

A new complex condensate was presented in [1]. This new solution is a periodic array of Shei's complex kink (4.5). Physically, it is associated with a crystalline phase of the NJL₂ system [1], just as the real kink crystal condensate (3.6) is associated with a crystalline phase of the GN₂ system [7]. Up to a plane-wave factor (as in Sec. IVA), this complex crystalline condensate is the general solution to the NLSE (2.13), and all other solutions (both real and complex) can be obtained from it by suitable choices of parameters. This solution can be written [43] in terms of

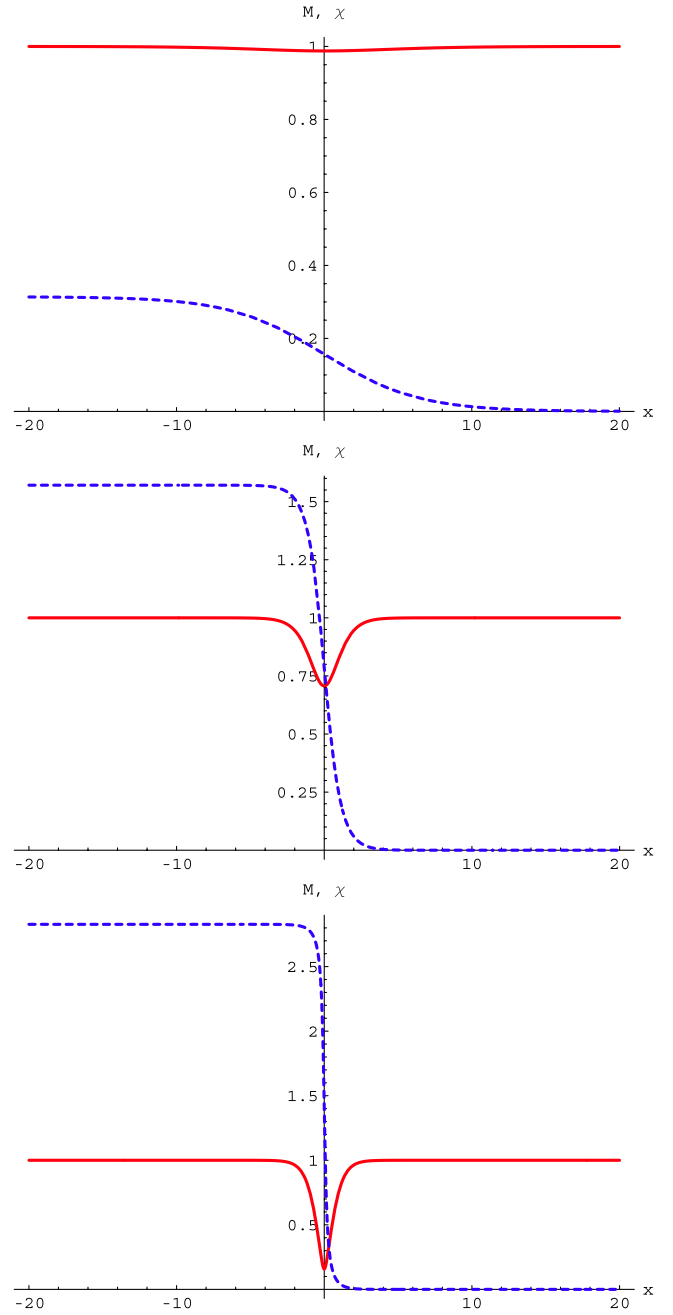


FIG. 5 (color online). Plots of the amplitude M and phase χ of the complex kink condensate (4.5), for three different values of the winding parameter θ . The condensate amplitude $M(x)$ (solid, red curves) approaches m at $x = \pm\infty$, and equals $m \cos(\theta/2)$ at the kink center $x = 0$. The phase $\chi(x)$ (dashed, blue curves) winds from θ to 0 as x ranges from $x = -\infty$ to $x = +\infty$. The plots are for $\theta = \pi/10$, $\theta = \pi/2$, and $\theta = 9\pi/10$.

Weierstrass elliptic functions (or, alternatively but equivalently, in terms of Jacobi theta functions),

$$\Delta(x) = -A \frac{\sigma(Ax + i\mathbf{K}' - i\theta/2)}{\sigma(Ax + i\mathbf{K}')\sigma(i\theta/2)} \exp[iAx(-i\zeta(i\theta/2) + \text{ins}(i\theta/2)) + i\theta\eta_3/2]. \quad (4.12)$$

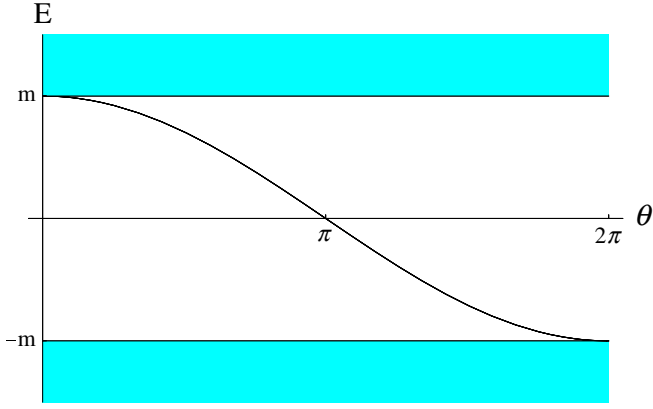


FIG. 6 (color online). Plot of the fermion single-particle spectrum for the single complex kink (4.5), as a function of the winding parameter θ . Note that for $\theta = \pi$ (when the condensate is real) the bound state is at 0, but for all other values of θ the bound state lies asymmetrically in the gap.

The parameter A sets the scale of the condensate and its length scale:

$$A = A(m, \theta, \nu) \equiv -2imsc(i\theta/4)nd(i\theta/4) \quad (4.13)$$

where $sc = sn/cn$ and $nd = 1/dn$ are Jacobi elliptic functions [37,38]. The functions σ and ζ are the Weierstrass sigma and zeta functions [37–40], some relevant properties of which are given in Appendix B. We have chosen real and imaginary half-periods: $\omega_1 = \mathbf{K}(\nu)$ and $\omega_3 = i\mathbf{K}' \equiv i\mathbf{K}(1-\nu)$. Both periods are therefore controlled by the single (real) elliptic parameter $0 \leq \nu \leq 1$. Also, $\eta_3 \equiv \zeta(i\mathbf{K}')$ is purely imaginary. The parameter $\theta \in [0, 4\mathbf{K}'(\nu)]$ is related to the angle through which the condensate rotates in one period $L = 2\mathbf{K}/A$:

$$\Delta(x + L) = e^{2i\varphi} \Delta(x) \quad (4.14)$$

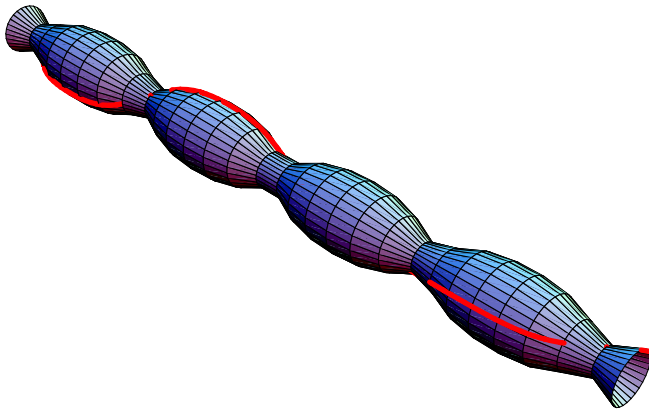


FIG. 7 (color online). Plot of the complex kink crystal condensate (4.12), for $\nu = 0.8$ and $\theta = 3\mathbf{K}(0.2)/2$, illustrating how the kink winds around zero each period, without the amplitude vanishing. The kink is the solid (red) line, and the surface is shown simply to illustrate that both the amplitude and the phase are changing over each period.

where the angle φ is a function of θ and ν ,

$$\varphi = \mathbf{K} \left(-i\zeta(i\theta/2) + ins(i\theta/2) - \frac{\eta\theta}{2\mathbf{K}} \right). \quad (4.15)$$

Here we used the quasiperiodicity property (B2) of the σ function. Note that φ and $\eta \equiv \zeta(\mathbf{K})$ are real, and when $\nu \rightarrow 1$, we have $\varphi \rightarrow -\theta/2$. This crystalline complex kink is plotted in Fig. 7, showing the winding of the kink over a period.

It is also useful to visualize the condensate (4.12) in terms of its amplitude and phase: $\Delta = M e^{i\chi}$. The modulus squared is a bounded periodic function, with period $2\mathbf{K}/A$:

$$M^2 \equiv |\Delta(x)|^2 = A^2 (\mathcal{P}(Ax + i\mathbf{K}') - \mathcal{P}(i\theta/2)). \quad (4.16)$$

Here we used the quasiperiodicity property (B2) of the σ function, together with the product identity (B12) relating the σ and \mathcal{P} functions. The phase χ can be expressed as

$$\chi(x) = A(-i\zeta(i\theta/2) + ins(i\theta/2))x + \frac{i}{2} \ln \left(\frac{\sigma(Ax + i\mathbf{K}' + i\theta/2)}{\sigma(Ax + i\mathbf{K}' - i\theta/2)} \right) + \frac{\eta_3 \theta}{2}. \quad (4.17)$$

The amplitude and phase are plotted in Fig. 8. Note that the amplitude is periodic while the phase changes by 2φ over each period.

The complex crystalline condensate in (4.12) satisfies the NLSE:

$$\Delta'' - 2|\Delta|^2\Delta - i(2Ains(i\theta/2))\Delta' - A^2(3\mathcal{P}(i\theta/2) - ns^2(i\theta/2))\Delta = 0. \quad (4.18)$$

Comparing this equation with the NLSE (2.13), we can extract the functions $a(E)$, $b(E)$, and $\mathcal{N}(E)$ appearing in (2.12), thereby determining the *exact* diagonal resolvent. To express these functions in a compact form, we define some properties of the associated fermionic spectrum for the BdG equation (1.8). This spectrum has positive and negative energy continua starting at $E = \pm m$, together with a single bound band in the gap, as depicted in Fig. 9. In contrast to the case for the real kink crystal in Sec. III, here the bound band is not centered in the middle of the gap, but is displaced from the center. The parameter θ characterizes this asymmetry in the spectrum. The band edges are functions of both the winding angle θ and the elliptic parameter ν :

$$\begin{aligned} E_1 &= -m, & E_2 &= m(-1 + 2nc^2(i\theta/4; \nu)), \\ E_3 &= m(-1 + 2nd^2(i\theta/4; \nu)), & E_4 &= +m. \end{aligned} \quad (4.19)$$

In the infinite period limit ($\nu \rightarrow 1$), the band contracts to a single bound state, with $E_2 = E_3 = m \cos(\theta/2)$, and this is precisely the bound state of the single complex kink, as shown in Fig. 6. At a finite period, but when $\theta = 2\mathbf{K}'(\nu)$, we find $E_2 = -E_3 = -\left(\frac{1-\sqrt{\nu}}{1+\sqrt{\nu}}\right)m$, and the band is centered symmetrically about 0; this is precisely the band spectrum of the real kink array in Sec. III. Thus, we can roughly

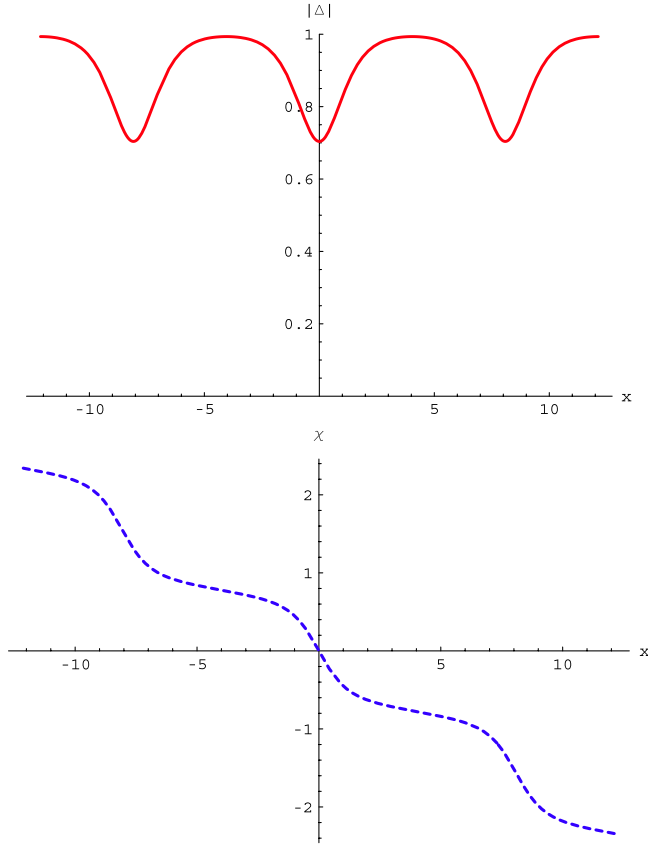


FIG. 8 (color online). Plots of the amplitude $M(x)$ and phase $\chi(x)$ of the complex kink crystal condensate (4.12), for $\theta = 1.6$ and $\nu = 0.95$.

think of the parameter θ as setting the offset location of the band inside the gap, while the parameter ν , together with θ , plays the role of determining the period of the crystal, and hence the width of the band. In terms of the band edges, the resolvent functions $a(E)$, $b(E)$, and $\mathcal{N}(E)$ that appear in the resolvent (2.12) take the following simple form [44]:

$$\begin{aligned} a(E) &= 2E^2 - (E_2 + E_3)E - \frac{(E_2 - E_3)^2}{4} - m^2, \\ b(E) &= 2E - (E_2 + E_3), \\ \mathcal{N}(E) &= \frac{1}{4\sqrt{(m^2 - E^2)(E - E_2)(E - E_3)}}. \end{aligned} \quad (4.20)$$

Here the normalization $\mathcal{N}(E)$ is fixed by the property $\det R = -\frac{1}{4}$.

1. Solution of NLSE by separation into amplitude and phase

We now comment on two ways to derive this solution to the NLSE (2.13). The first is to separate the NLSE into two equations, one for the amplitude and one for the phase. Writing $\Delta(x) = M(x)e^{i\chi(x)}$, and considering $(\Delta^* \Delta'' - \Delta''^* \Delta)$, we immediately find that the phase is related to

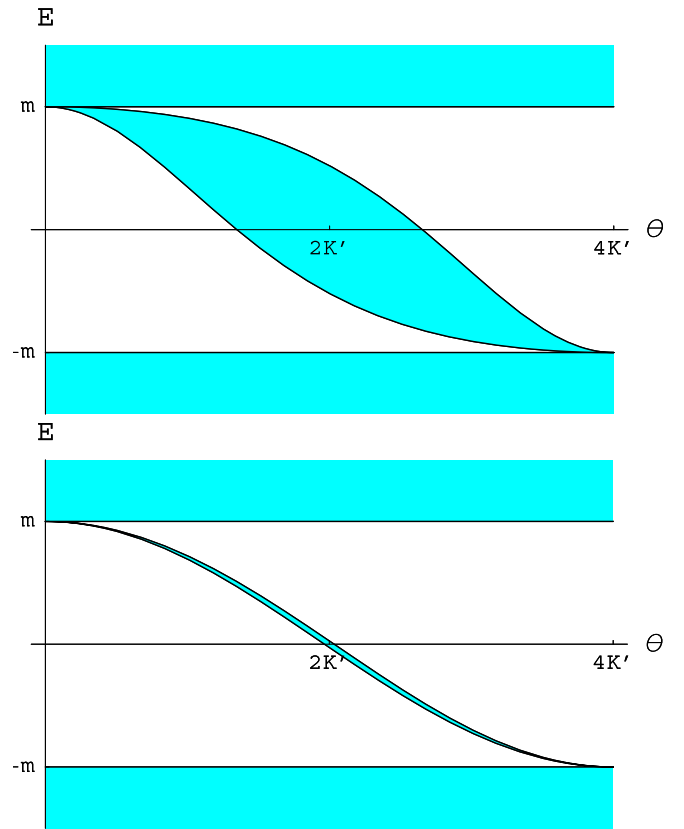


FIG. 9 (color online). Plots of the single-particle fermion spectrum for the complex kink crystal condensate (4.12), for $\nu = 0.1$ (first plot) and $\nu = 0.9$ (second plot), as a function of the winding parameter θ . Note that for $\theta = 2\mathbf{K}'$ (when the condensate is real) the band is centered symmetrically about $E = 0$, but for all other values of θ the band lies asymmetrically in the gap. In the infinite period limit, $\nu \rightarrow 1$, the bound band shrinks to a single bound state, and its θ dependence reduces to that depicted in Fig. 6 for the single complex kink condensate.

the amplitude by

$$\chi'(x) = -\frac{1}{2}(b - 2E) + \frac{C_1}{M^2(x)} \quad (4.21)$$

where C_1 is a constant. Note that this is indeed true for all the complex condensate solutions discussed above. For the crystalline complex solution in (4.16) and (4.17), the relation (4.21) can be verified using the Weierstrass function properties listed in Appendix B, in particular Eq. (B15).

Next, considering $(\Delta^* \Delta'' + \Delta''^* \Delta)$, we find the following nonlinear equation for M^2 :

$$\begin{aligned} ((M^2)')^2 &= 4M^6 + 2(4(a - Eb) - \frac{1}{2}(b - 2E)^2)M^4 \\ &\quad + C_2 M^2 - 4C_1^2 \end{aligned} \quad (4.22)$$

where C_2 is another constant. From the form of this equation, comparing with the equation (B10) for the Weierstrass \mathcal{P} function [37–40], we recognize the solution

to be of the form

$$M^2 = A^2[\mathcal{P}(Ax + i\mathbf{K}') - \mathcal{P}(C_3)]. \quad (4.23)$$

The shift by $i\mathbf{K}'$ ensures that $M^2(x)$ is bounded for x on the real axis. This explains the result in (4.16), identifying $C_3 = i\theta/2$. The constants C_1 and C_2 are related to C_3 as

$$C_1 = -\frac{i}{2}A^3\mathcal{P}'(i\theta/2), \quad C_2 = 2A^4\mathcal{P}''(i\theta/2). \quad (4.24)$$

Given this solution for the amplitude, the phase follows from (4.21), using the integration formula [37]

$$\begin{aligned} & \frac{1}{A} \int \frac{\mathcal{P}'(C_3)}{\mathcal{P}(Ax + i\mathbf{K}') - \mathcal{P}(C_3)} dx \\ &= \ln\left(\frac{\sigma(Ax + i\mathbf{K}' - C_3)}{\sigma(Ax + i\mathbf{K}' + C_3)}\right) + 2(Ax + i\mathbf{K}')\zeta(C_3). \end{aligned} \quad (4.25)$$

Notice that the phase can always be shifted by qx , which amounts to multiplying the solution by a plane-wave factor, as discussed in Sec. IV A. In our solution (4.12), the plane-wave factor has been chosen so that the associated fermion spectrum has the form shown in Fig. 9. An additional plane-wave factor in $\Delta(x)$ displaces this entire spectrum by a constant.

2. Solution of NLSE as a periodic array of complex kinks

Another way to derive the general periodic complex solution to the NLSE is to make an educated guess for a periodic array of Shei's complex kink solution (4.5), using known properties of the Weierstrass functions. Shei's complex kink condensate (4.5) can be written as

$$\Delta(x) = m \frac{\sinh(m \sin(\theta/2)x + i\pi/2 - i\theta/2)}{\sinh(m \sin(\theta/2)x + i\pi/2)} e^{i\theta/2}. \quad (4.26)$$

This can be made quasiperiodic along the real x axis by generalizing the hyperbolic sine function to its doubly periodic form, which is the Weierstrass sigma function. Thus, we are led to try the form

$$\Delta(x) = A e^{i\theta\eta_3/2} \frac{\sigma(Ax + i\mathbf{K}' - i\theta/2)}{\sigma(Ax + i\mathbf{K}')\sigma(i\theta/2)} e^{i\lambda x} \quad (4.27)$$

where we have included a possible plane-wave factor $e^{i\lambda x}$, to be determined, and the normalization factors $\frac{e^{i\theta\eta_3/2}}{\sigma(i\theta/2)}$ have been chosen for convenience.

Given this form of $\Delta(x)$, since $\zeta(x) \equiv d/dx \ln \sigma(x)$, we find

$$\Delta' = A\{\zeta(Ax + i\mathbf{K}' - i\theta/2) - \zeta(Ax + i\mathbf{K}') + i\lambda/A\}\Delta, \quad (4.28)$$

and since $\mathcal{P} \equiv -\zeta'$, we find

$$\begin{aligned} \Delta'' &= A^2\{[-\mathcal{P}(Ax + i\mathbf{K}' - i\theta/2) + \mathcal{P}(Ax + i\mathbf{K}')] \\ &+ [\zeta(Ax + i\mathbf{K}' - i\theta/2) \\ &- \zeta(Ax + i\mathbf{K}') + i\lambda/A]^2\}\Delta. \end{aligned} \quad (4.29)$$

Furthermore, using the quasiperiodicity properties of the Weierstrass functions (B2) and the Weierstrass function product formula (B12), it follows that

$$\begin{aligned} |\Delta(x)|^2 &= A^2 \frac{\sigma(Ax + i\mathbf{K}' - i\theta/2)\sigma(Ax + i\mathbf{K}' + i\theta/2)}{\sigma^2(Ax + i\mathbf{K}')\sigma(i\theta/2)\sigma(-i\theta/2)} \\ &= A^2[\mathcal{P}(Ax + i\mathbf{K}') - \mathcal{P}(i\theta/2)]. \end{aligned} \quad (4.30)$$

Therefore,

$$\begin{aligned} \Delta'' - 2|\Delta|^2\Delta &= A^2\{-[\mathcal{P}(Ax + i\mathbf{K}' - i\theta/2) \\ &+ \mathcal{P}(Ax + i\mathbf{K}')] + [\zeta(Ax + i\mathbf{K}' - i\theta/2) \\ &- \zeta(Ax + i\mathbf{K}') + i\lambda/A]^2 + 2\mathcal{P}(i\theta/2)\}\Delta \end{aligned} \quad (4.31)$$

where we note that the relative sign between the first \mathcal{P} functions has been flipped by the subtraction of $2|\Delta|^2\Delta$.

Now we use the remarkable identity (B14) that relates the \mathcal{P} function to squares of the ζ function, to find that

$$\begin{aligned} \Delta'' - 2\Delta^2\Delta &= A^2[3\mathcal{P}(i\theta/2) + (\lambda/A + i\zeta(i\theta/2))^2]\Delta \\ &+ 2iA[\lambda/A + i\zeta(i\theta/2)]\Delta'. \end{aligned} \quad (4.32)$$

Thus, $\Delta(x)$ of the form in (4.27) does indeed satisfy the NLSE (2.13), and one simply needs to match the constants algebraically in order to express $a(E)$, $b(E)$, and $\mathcal{N}(E)$ in terms of θ . This determines λ in (4.27) up to an additive constant, which can be fixed by matching the fermion spectrum to the form in (4.19).

D. Reduction of the general solution to special cases

To conclude this section describing our new complex crystalline solution (4.12), we note that it incorporates all previously known solutions as special cases.

1. Reduction to the real kink crystal condensate

When $\theta = 2\mathbf{K}'$, the scale factor $A \rightarrow 2m/(1 + \sqrt{\nu})$, and the condensate reduces to the real kink crystal in (3.6):

$$\begin{aligned} \Delta &\rightarrow \frac{2m\sqrt{\nu}}{1 + \sqrt{\nu}} \operatorname{sn}\left(\frac{2mx}{1 + \sqrt{\nu}}; \nu\right) = m\tilde{\nu} \frac{\operatorname{sn}(mx; \tilde{\nu})\operatorname{cn}(mx; \tilde{\nu})}{\operatorname{dn}(mx; \tilde{\nu})}, \\ \tilde{\nu} &= \frac{4\sqrt{\nu}}{(1 + \sqrt{\nu})^2}. \end{aligned} \quad (4.33)$$

In this limit, the amplitude vanishes at $x = 0$, and one sees that the kink ‘‘winds’’ through the angle $2\varphi = -\pi$ by passing through zero. For other values of θ , the complex kink crystal winds around zero, but without the amplitude

actually vanishing. For $\theta = 2\mathbf{K}'$, the bound band becomes symmetric about $E = 0$, because the band edges (4.19) reduce to

$$E_2 \rightarrow -m \left(\frac{1 - \sqrt{\nu}}{1 + \sqrt{\nu}} \right), \quad E_3 \rightarrow m \left(\frac{1 - \sqrt{\nu}}{1 + \sqrt{\nu}} \right). \quad (4.34)$$

Accordingly, the resolvent functions $a(E)$, $b(E)$, and $\mathcal{N}(E)$ in (4.20) reduce smoothly when $\theta = 2\mathbf{K}'$ to the corresponding expressions for the real kink crystal in (3.10).

2. Reduction to the single complex kink condensate

For general θ , when $\nu \rightarrow 1$, the complex crystalline condensate in (4.12) reduces to Shei's complex kink solution (4.5). To see this, first observe that in this limit, $A(m, \theta, \nu) \rightarrow m \sin(\theta/2)$, and \mathbf{K} diverges, while $\mathbf{K}' \rightarrow \pi/2$. Thus the period $2\mathbf{K}/A$ diverges. Also, the band edges contract as $E_2 \rightarrow E_3 = m \cos(\theta/2)$, so the band shrinks to a single bound state, whose θ dependence matches that of the bound state for Shei's complex kink condensate. Furthermore, as $\nu \rightarrow 1$, the Weierstrass functions simplify:

$$\begin{aligned} \sigma(x) &\rightarrow \sinh(x)e^{-x^2/6}, & \zeta(x) &\rightarrow -\frac{x}{3} + \coth(x), \\ \mathcal{P}(x) &\rightarrow \frac{1}{3} + \frac{1}{\sinh^2(x)}. \end{aligned} \quad (4.35)$$

These relations show that on the interval $[-\mathbf{K}/A, \mathbf{K}/A]$, in the limit $\nu \rightarrow 1$, the complex crystalline condensate (4.12) reduces to Shei's single complex kink condensate (4.5) up to an unimportant constant phase factor.

3. Reduction to the single plane-wave condensate

In the opposite limit, as $\nu \rightarrow 0$, the period remains finite because $\mathbf{K} \rightarrow \pi/2$ and $A \rightarrow 2 \tanh(\theta/4)$. As $\nu \rightarrow 0$, the

Weierstrass functions simplify:

$$\begin{aligned} \sigma(x) &\rightarrow \sin(x)e^{x^2/6}, & \zeta(x) &\rightarrow \frac{x}{3} + \cot(x), \\ \mathcal{P}(x) &\rightarrow -\frac{1}{3} + \frac{1}{\sin^2(x)}. \end{aligned} \quad (4.36)$$

Thus, the complex crystalline condensate (4.12) reduces to a single plane-wave (chiral spiral) form:

$$\Delta \rightarrow m \operatorname{sech}^2(\theta/4) e^{-2im \tanh^2(\theta/4)x}. \quad (4.37)$$

V. SOLUTIONS TO THE BOGOLIUBOV/DE GENNES EQUATION

A. Spinor solutions

Remarkably, not only is it possible to solve the NLSE (2.13) exactly, we can also solve exactly the associated BdG equation [45]. In the previous sections we described the spectrum; here we present the explicit spinor solutions and express the spectral information in a more compact and useful form. We write the BdG equation (1.8) as

$$\begin{pmatrix} -i \frac{d}{dx} & \Delta(x) \\ \Delta^*(x) & i \frac{d}{dx} \end{pmatrix} \psi = E \psi. \quad (5.1)$$

The solutions for the real condensates in Sec. III are well known [3,6]. For the complex plane wave, $\Delta(x) = Ae^{iqx}$, the solutions are simply chiral rotations of free spinors, and are discussed, for example, in [46]. For Shei's complex kink condensate (4.5), the spinor solutions are given in [4,47]. For the complex kink crystal (4.12), the two independent spinor solutions can be written as

$$\begin{aligned} \psi_- &= \sqrt{\frac{A}{2|dk/d\alpha|}} e^{-i\eta_3 \alpha} \begin{pmatrix} \frac{\sigma(Ax+i\mathbf{K}'+i\alpha-i\theta/4)}{\sigma(Ax+i\mathbf{K}')\sigma(i\alpha-i\theta/4)} e^{(iAx/2)[-i\zeta(i\theta/2)+\operatorname{ins}(i\theta/2)]+i\theta\eta_3/4+i\pi/4} \\ \frac{\sigma(Ax+i\mathbf{K}'+i\alpha+i\theta/4)}{\sigma(Ax+i\mathbf{K}')\sigma(i\alpha+i\theta/4)} e^{-(iAx/2)[-i\zeta(i\theta/2)+\operatorname{ins}(i\theta/2)]-i\theta\eta_3/4-i\pi/4} \end{pmatrix} e^{(iAx/2)[i\zeta(i\alpha+i\theta/4)+i\zeta(i\alpha-i\theta/4)]}, \\ \psi_+ &= -\sqrt{\frac{A}{2|dk/d\alpha|}} e^{i\eta_3 \alpha} \begin{pmatrix} \frac{\sigma(Ax+i\mathbf{K}'-i\alpha-i\theta/4)}{\sigma(Ax+i\mathbf{K}')\sigma(i\alpha+i\theta/4)} e^{(iAx/2)[-i\zeta(i\theta/2)+\operatorname{ins}(i\theta/2)]+i\theta\eta_3/4+i\pi/4} \\ \frac{\sigma(Ax+i\mathbf{K}'-i\alpha+i\theta/4)}{\sigma(Ax+i\mathbf{K}')\sigma(i\alpha-i\theta/4)} e^{-(iAx/2)[-i\zeta(i\theta/2)+\operatorname{ins}(i\theta/2)]-i\theta\eta_3/4-i\pi/4} \end{pmatrix} e^{-i(Ax/2)[i\zeta(i\alpha+i\theta/4)+i\zeta(i\alpha-i\theta/4)]}. \end{aligned} \quad (5.2)$$

Here, α is a spectral parameter that characterizes the energy and momentum of these solutions, and k is the momentum, defined below in (5.7). Notice that ψ_{\pm} differ from one another by the sign of α .

To relate the energy eigenvalue E to the spectral parameter α , we substitute these forms into the BdG equation (5.1), and make use of the Weierstrass function identity (B13). This identity immediately shows that these are indeed solutions, and determines the energy to be

$$\begin{aligned} E(\alpha) &= \frac{A}{2} [i\zeta(i\alpha - i\theta/4) - i\zeta(i\alpha + i\theta/4) \\ &\quad + i\zeta(i\theta/2) + \operatorname{ins}(i\theta/2)] \\ &= -m + 2m \left(\frac{\mathcal{P}(i\theta/4) - \mathcal{P}(i\mathbf{K}')}{\mathcal{P}(i\theta/4) - \mathcal{P}(i\alpha)} \right) \end{aligned} \quad (5.3)$$

where A is given by (4.13). The spectral parameter α is defined on the vertical edges, $0 \leq i\alpha \leq i\mathbf{K}'(\nu)$,

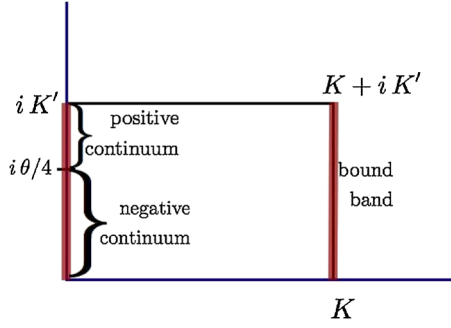


FIG. 10 (color online). The fundamental rectangle for the spectral parameter $i\alpha$ appearing in the spinor solutions (5.2) to the BdG equation. The bound band is characterized by $\mathbf{K}(\nu) \leq i\alpha \leq \mathbf{K}(\nu) + i\mathbf{K}'(\nu)$, while the positive and negative energy continua are characterized by $0 \leq i\alpha \leq i\mathbf{K}'(\nu)$. The point $\alpha = \theta/4$ represents $E = \pm\infty$, depending on the side of approach.

$\mathbf{K}(\nu) \leq i\alpha \leq \mathbf{K}(\nu) + i\mathbf{K}'(\nu)$, of the fundamental rectangle shown in Fig. 10. Only on these edges of the fundamental rectangle are the spinor wave functions in (5.2) bounded, and is the energy $E(\alpha)$ real. The vertices of the rectangle correspond to the band edges [compare with Eq. (4.19)]:

$$\begin{aligned} E_1 &= E(i\alpha = 0) = -m, \\ E_2 &= E(i\alpha = \mathbf{K}) = m(-1 + 2nc^2(i\theta/4)), \\ E_3 &= E(i\alpha = \mathbf{K} + i\mathbf{K}') = m(-1 + 2nd^2(i\theta/4)), \\ E_4 &= E(i\alpha = i\mathbf{K}') = +m. \end{aligned} \quad (5.4)$$

The right-hand boundary of the fundamental rectangle corresponds to the bound band, while the left-hand boundary corresponds to the positive and negative energy continua. The point $\alpha = \theta/4$ is associated with the point at infinity; the bottom of the Dirac sea is approached as $\alpha \rightarrow \theta/4$ from below, and the top of the positive energy continuum as $\alpha \rightarrow \theta/4$ from above. This is depicted in Fig. 11.

To identify the momentum associated with these solutions, we recall that the quasiperiodic winding (4.14) of the condensate in (4.12) implies that the BdG Hamiltonian (1.7) is invariant under a period shift, up to a global chiral rotation through the winding angle φ :

$$H(x + L) = e^{i\gamma_5\varphi} H(x) e^{-i\gamma_5\varphi}. \quad (5.5)$$

Using the quasiperiodicity properties of the Weierstrass functions (B2), we see that under a period shift, the spinors in (5.2) acquire a chiral rotation and a Bloch phase:

$$\psi_{\pm}(x + L) = e^{\pm ikL} e^{i\varphi\gamma_5} \psi_{\pm}(x) \quad (5.6)$$

where φ is the winding angle defined in (4.15). The Bloch momentum k is expressed in terms of the spectral parameter α as

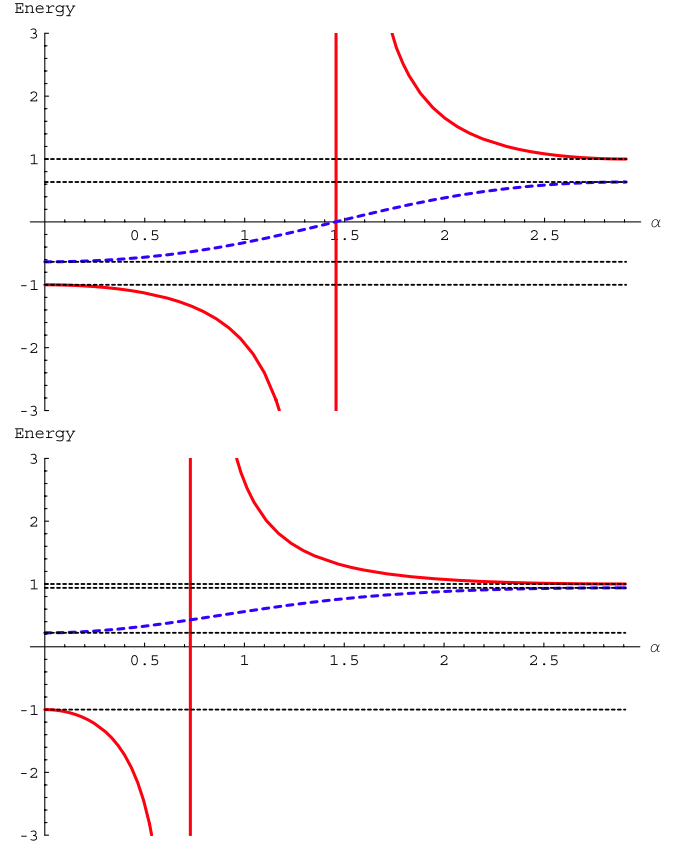


FIG. 11 (color online). Energy $E(\alpha)$ from (5.3) as a function of the spectral parameter α , for two different values of θ . The solid (red) curves show the continuum energies, while the dashed (blue) curves show the energy in the bound band. The horizontal dashed lines denote the band edge energies $E_1, E_2, E_3,$ and E_4 from (5.4), and the vertical (red) line gives the asymptote to $E = \mp\infty$ at $\alpha = \theta/4$, as discussed in the text. These curves are for the elliptic parameter $\nu = 0.05$. The first plot is for $\theta = 2\mathbf{K}' = 5.82$, so that the band is symmetric about the origin. The second plot is for $\theta = \mathbf{K}' = 2.91$, so the band is asymmetrically offset from the origin.

$$k(\alpha) = -\frac{A}{2} [i\zeta(i\alpha + i\theta/4) + i\zeta(i\alpha - i\theta/4) + 2\eta\alpha/\mathbf{K}]. \quad (5.7)$$

This is the relativistic version of Bloch's theorem. The momentum is real for α taking values on the vertical edges of the fundamental rectangle, and is plotted in Fig. 12. Since $k(\alpha)$ is odd in α , we see that ψ_{\pm} in (5.2) are positive and negative momentum solutions.

B. Density of states

In this section we present an efficient characterization of the density of states, and show how this relates to the resolvent in (2.12). In the previous section, both the energy E and the momentum k were expressed in terms of the spectral parameter α . Now consider the derivatives of the energy and momentum with respect to the spectral parame-

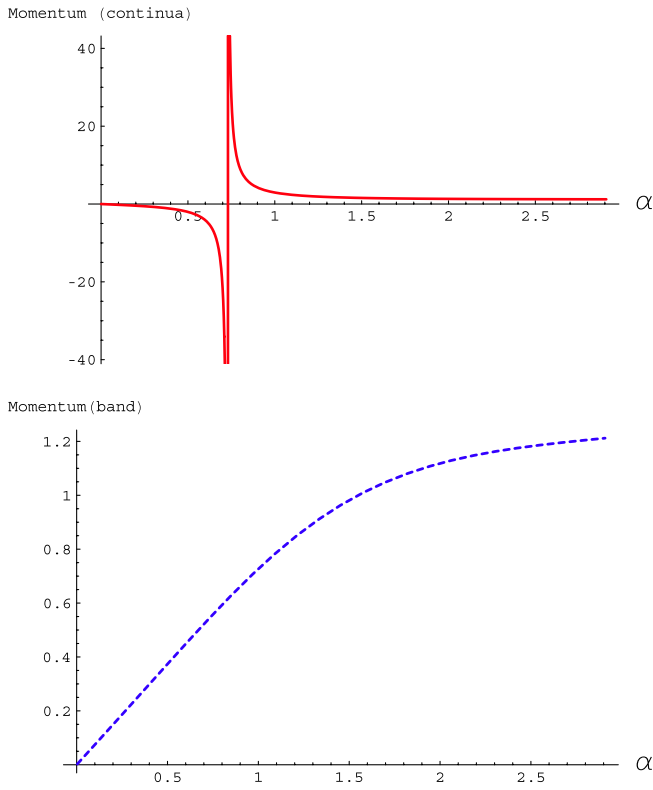


FIG. 12 (color online). Momentum as a function of the spectral parameter α , in the positive and negative continua (first plot) and in the bound band (second plot). Note that $dk/d\alpha$ is negative in the continuum and positive in the bound band. These plots are for $\nu = 0.05$ and $\theta = \mathbf{K}'$, as in the second panel in Fig. 11. The vertical (red) line in the first plot gives the asymptote to $k = \mp\infty$ at $\alpha = \theta/4$, as discussed in the text.

ter α . From (5.3) and (5.7) we see that

$$\begin{aligned} \frac{dE}{d\alpha} &= -\frac{A}{2}[\mathcal{P}(i\alpha + i\theta/4) - \mathcal{P}(i\alpha - i\theta/4)], \\ \frac{dk}{d\alpha} &= -\frac{A}{2}[\mathcal{P}(i\alpha + i\theta/4) + \mathcal{P}(i\alpha - i\theta/4) + 2\eta/\mathbf{K}]. \end{aligned} \quad (5.8)$$

The significance of these expressions becomes clearer once we write the resolvent functions $a(E)$, $b(E)$, and $\mathcal{N}(E)$ in (4.20) as functions of α (instead of E):

$$a(\alpha) = \frac{A^2}{2}[2\mathcal{P}(i\theta/2) - \mathcal{P}(i\alpha + i\theta/4) - \mathcal{P}(i\alpha - i\theta/4)], \quad (5.9)$$

$$\begin{aligned} b(\alpha) &= A[i\zeta(i\alpha - i\theta/4) - i\zeta(i\alpha + i\theta/4) \\ &\quad + i\zeta(i\theta/2) - \text{ins}(i\theta/2)], \end{aligned} \quad (5.10)$$

$$\mathcal{N}(\alpha) = \frac{\mp i}{A^2[\mathcal{P}(i\alpha + i\theta/4) - \mathcal{P}(i\alpha - i\theta/4)]}. \quad (5.11)$$

Here the upper sign in \mathcal{N} is for the continuum states, and

the lower sign is for the band. Thus, we recognize $dE/d\alpha$ as

$$\frac{dE}{d\alpha} = \mp \frac{2}{A} \sqrt{(E^2 - m^2)(E - E_2)(E - E_3)}. \quad (5.12)$$

And $dk/d\alpha$ can be written as

$$\frac{dk}{d\alpha} = -A[\mathcal{P}(i\theta/2) - a(\alpha)/A^2 + \eta/\mathbf{K}], \quad (5.13)$$

which is negative in the continuum and positive in the band (see Fig. 12). Consequently, the density of states can be expressed as

$$\frac{dk}{dE} = \frac{dk/d\alpha}{dE/d\alpha} = \mp \frac{[a(E) - A^2\mathcal{P}(i\theta/2) - A^2\eta/\mathbf{K}]}{2\sqrt{(E^2 - m^2)(E - E_2)(E - E_3)}}. \quad (5.14)$$

When $\theta = 2\mathbf{K}'$, which is the GN_2 limit (i.e., with a real condensate), this density of states reduces to

$$\begin{aligned} \frac{dk}{dE} &= \mp \frac{E^2 - m^2 \frac{E(\tilde{\nu})}{\mathbf{K}(\tilde{\nu})}}{\sqrt{(E^2 - m^2)(E^2 - m^2(1 - \tilde{\nu}))}}, \\ \tilde{\nu} &\equiv \frac{4\sqrt{\nu}}{(1 + \sqrt{\nu})^2} \end{aligned} \quad (5.15)$$

where \mathbf{E} and \mathbf{K} are the complete elliptic integrals [37,38]. This density of states (5.15) is precisely that found for the single-band finite-gap Schrödinger system of the GN_2 model [7]. The result in (5.14) generalizes this density of states to the general complex crystalline condensate (4.12).

The density of states (5.14) has been derived from the energy and momentum of the spinor solutions in (5.2). For consistency, we compare this with the trace of the resolvent (2.12) over one period:

$$\begin{aligned} \frac{1}{L} \int_L \text{tr}_D R(x; E) dx &= \frac{A}{2\mathbf{K}} \int_{-\mathbf{K}/A}^{+\mathbf{K}/A} 2\mathcal{N}(E)(a(E) + |\Delta(x)|^2) dx \\ &= \frac{A\mathcal{N}(E)}{\mathbf{K}} \int_{-\mathbf{K}/A}^{+\mathbf{K}/A} dx [a(E) \\ &\quad + A^2(\mathcal{P}(Ax + i\mathbf{K}') - \mathcal{P}(i\theta/2))] \\ &= \frac{[a(E) - A^2\mathcal{P}(i\theta/2) - A^2\eta/\mathbf{K}]}{2\sqrt{(m^2 - E^2)(E - E_2)(E - E_3)}}, \end{aligned} \quad (5.16)$$

where we have used the integral

$$\int_{-\mathbf{K}/A}^{+\mathbf{K}/A} \mathcal{P}(Ax + i\mathbf{K}') dx = -\frac{2\eta}{A}. \quad (5.17)$$

This illustrates the consistency of our resolvent ansatz (2.12) with the spectral properties of the associated BdG equation.

VI. HARTREE-FOCK APPROACH AND THE GAP EQUATION

So far we have shown that the gap equation (1.4) can be reduced to the NLSE (2.13), and we have found the general solution to the NLSE. We now show the self-consistency of this approach by verifying that the gap equation in the form (2.9) is indeed satisfied. Inserting our ansatz form (2.12) for the resolvent, the gap equation in this form reads

$$\Delta(x) = -2iNg^2 \text{tr}_E[\mathcal{N}(E)(b(E)\Delta(x) - i\Delta'(x))]. \quad (6.1)$$

To verify (6.1), we require information about the single-particle fermionic spectrum of the BdG Hamiltonian for the condensate $\Delta(x)$ that we have found. This provides a complementary approach to finding a self-consistent condensate, by solving the associated relativistic Hartree-Fock problem.

A. Solving the gap equation from the resolvent

We first need to show that the coefficient of $\Delta'(x)$ on the right-hand side of (6.1) vanishes once the energy trace is taken:

$$\text{tr}_E[\mathcal{N}(E)] = 0. \quad (6.2)$$

This computation is greatly simplified by converting it into an integral over the spectral parameter α . Recalling (5.12) and the normalization factor in (4.20), we have

$$\mathcal{N}(E) = \pm \frac{i}{2A} \frac{d\alpha}{dE}. \quad (6.3)$$

We assume that the negative energy continuum is fully occupied, and that the band inside the gap is partially occupied, by a fraction ξ . Then we can express (6.2) as

$$\begin{aligned} 0 &= \frac{i}{2\pi A} \left\{ \int_0^{\theta/4} d\alpha - \int_{-i\mathbf{K}}^{-i\mathbf{K}+\xi\mathbf{K}'} d\alpha \right\} \\ &= \frac{i}{2\pi A} (\theta/4 - \xi\mathbf{K}'). \end{aligned} \quad (6.4)$$

$$\bar{\psi}_k(x)\psi_k(x) - i\bar{\psi}_k(x)i\gamma^5\psi_k(x) = \psi_k^\dagger(x)(\gamma^0 + \gamma^1)\psi_k(x)$$

$$\begin{aligned} &= \frac{iA}{|dk/d\alpha|} e^{-2i\eta_3\alpha} e^{iA\alpha[-i\zeta(i\theta/2)+\text{ins}(i\theta/2)]} \frac{\sigma(Ax+i\mathbf{K}'+i\alpha-i\theta/4)\sigma(Ax-i\mathbf{K}'-i\alpha-i\theta/4)}{\sigma(Ax+i\mathbf{K}')\sigma(-i\alpha-i\theta/4)\sigma(i\alpha-i\theta/4)\sigma(Ax-i\mathbf{K}')} \\ &= \frac{i}{|dk/d\alpha|} [\zeta(Ax+i\mathbf{K}') + \zeta(i\alpha-i\theta/4) - \zeta(Ax+i\mathbf{K}'-i\theta/2) - \zeta(i\alpha+i\theta/4)]\Delta(x) \\ &= \frac{1}{|dk/d\alpha|} \frac{1}{A} [b(E)\Delta(x) - i\Delta'(x)] \end{aligned} \quad (6.7)$$

where the subscript k on ψ emphasizes that these are spinor solutions of a given momentum k . In deriving (6.7) we have used the product identity (B13) for the Weierstrass sigma function.

Thus, θ must satisfy the condition

$$\frac{\theta}{4\mathbf{K}'} = \xi = \text{filling fraction}. \quad (6.5)$$

This filling fraction condition is depicted in Fig. 13.

To appreciate this condition, we consider some special limiting cases. In the real (GN_2) limit, where $\theta = 2\mathbf{K}'$, this corresponds to filling the band halfway. Since the band is symmetrically placed about zero energy, this corresponds precisely to filling all the negative energy states, as in the conventional GN_2 model analysis [2,3]. For the single kink, which is obtained in the infinite period limit, the bound state is half occupied [28,30].

For general θ , in the infinite period limit, where $\mathbf{K}' \rightarrow \pi/2$, we recover Shei's condition (4.11) that $\theta/2\pi$ is the fractional filling of the bound state in the gap. Note that in this case, the fractional filling of this state is conventionally interpreted [4,5] in terms of the filling of the level by a fixed fraction $\frac{n}{N}$ of the fermion flavors, with this fraction kept fixed in the infinite N limit. At a finite period, it is thermodynamically more natural to consider a fraction of the band being occupied by all flavors, as above. As the band contracts to a single bound state in the infinite period limit, we smoothly tend to the situation of having the level partially filled, while maintaining consistency with the gap equation for any period.

The other condition required for the gap equation (6.1) to be satisfied is that

$$-2iNg^2 \text{tr}_E[\mathcal{N}(E)b(E)] = 1. \quad (6.6)$$

This is the standard vacuum gap equation for the renormalization of the coupling [2–5].

B. Solving the gap equation from the spinor solutions

Given the spinor solutions of the BdG equation, we can reconstruct the expectation values $\langle \bar{\psi}(x)\psi(x) \rangle$ and $-\langle \bar{\psi}(x)i\gamma^5\psi(x) \rangle$, to verify that they correspond to the real and imaginary parts of the condensate $\Delta(x)$. From (5.2), we find

Thus, for a given momentum k , $\bar{\psi}_k(x)\psi_k(x) - i\bar{\psi}_k(x)i\gamma^5\psi_k(x)$ has the same x dependence as the upper off-diagonal entry of the resolvent, which appears in the gap equation (6.1). To compute the expectation value we

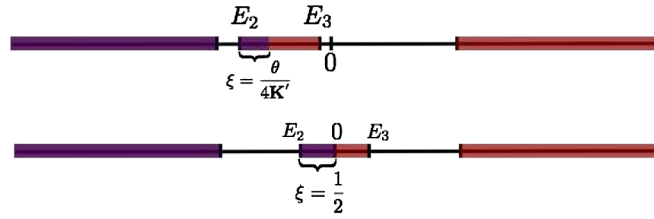


FIG. 13 (color online). The occupation of single-particle fermionic states for two different values of θ . In general, to satisfy the gap equation the condition (6.5) relates the condensate parameter θ to the filling fraction of the bound band. In the special case $\theta = 2\mathbf{K}'$, this filling fraction is $1/2$, and this corresponds to the real condensate of the discrete-chiral GN_2 model, for which the spectrum is symmetric about 0. Thus, in this case, all the negative energy states are filled.

trace over the N flavors and integrate over momentum:

$$\begin{aligned} \langle \bar{\psi}(x)\psi(x) \rangle - i\langle \bar{\psi}(x)i\gamma^5\psi(x) \rangle &= N \int \frac{dk}{2\pi} [\bar{\psi}_k(x)\psi_k(x) \\ &\quad - i\bar{\psi}_k(x)i\gamma^5\psi_k(x)] \\ &= \frac{N}{2\pi A} \int d\alpha \text{sgn}\left(\frac{dk}{d\alpha}\right) \\ &\quad \times [b(\alpha)\Delta(x) - i\Delta'(x)]. \end{aligned} \quad (6.8)$$

Thus we have precisely the same integrals as were evaluated in the previous section to show that the gap equation is satisfied. The vanishing of the coefficient of $\Delta'(x)$ leads to the same relation (6.5) between the filling fraction and θ , while the coefficient of $\Delta(x)$ is again the vacuum gap equation (6.6) expressing the renormalization of the coupling constant g .

It is interesting to note that while the condensate $\Delta(x)$ is spatially inhomogeneous, the expectation value of the charge density is spatially uniform. From the explicit spinor solutions in (5.2), we find

$$\psi_k^\dagger(x)\psi_k(x) = \frac{1}{|dk/d\alpha|} \frac{1}{A} (|\Delta(x)|^2 + a(\alpha)). \quad (6.9)$$

For a given single-particle state of momentum k , the charge density $\psi_k^\dagger(x)\psi_k(x)$ is spatially inhomogeneous, but this inhomogeneity is washed out by integrating over k , so that the expectation value is uniform:

$$\frac{d}{dx} \langle \psi^\dagger(x)\psi(x) \rangle = 0. \quad (6.10)$$

Indeed, for a given k , the charge density $\psi_k^\dagger(x)\psi_k(x)$ has spatial inhomogeneity determined by $|\Delta(x)|^2$, the magnitude squared of the condensate. But the coefficient of this x -dependent term in (6.9) is precisely the same as the coefficient of the $\Delta'(x)$ term in (6.7). We just saw above that this term vanishes (when the energy trace is taken), in order to satisfy the gap equation. Thus, the very same condition (6.5) that ensures that the gap equation is satisfied also shows that $\langle \psi^\dagger(x)\psi(x) \rangle$ is uniform.

There is another, more physical way to understand this fact [48]. It expresses the conservation of axial charge in

the NJL_2 model. Recall that the NJL_2 system has two conserved currents: the first is the charge current $j^\mu = \bar{\psi}\gamma^\mu\psi$, and the second is the axial current $j_5^\mu = \bar{\psi}\gamma^\mu\gamma^5\psi$. In $1+1$ dimensions these are related by $j_5^\mu = \epsilon^{\mu\nu}j_\nu$. For static but spatially inhomogeneous condensates, the charge current conservation is automatically satisfied. Axial current conservation is more interesting. For a static condensate,

$$\frac{\partial}{\partial x^\mu} \langle j_5^\mu(x) \rangle = \frac{d}{dx} \langle \psi^\dagger(x)\psi(x) \rangle \quad (6.11)$$

so axial charge conservation requires a uniform charge expectation value, as was found above in (6.10) from the single-particle spectral properties. Another way to see this is to observe that we can express the expectation value of the axial current in terms of the resolvent

$$\langle j_5^\mu \rangle = \text{tr}_{E,D}(\gamma^0\gamma^\mu\gamma^5 R(x; E)). \quad (6.12)$$

Taking the spatial derivative and using the Eilenberger equation (2.6), we find

$$\begin{aligned} \frac{d}{dx} \langle j_5^1 \rangle &= \text{tr}_{E,D}(\partial_x R(x; E)) \\ &= 2\sigma(x) \langle \bar{\psi}(x)i\gamma^5\psi(x) \rangle - 2\pi(x) \langle \bar{\psi}(x)\psi(x) \rangle. \end{aligned} \quad (6.13)$$

Thus, once again, the gap equation ensures that axial current conservation is satisfied. Interestingly, it is encoded into the Eilenberger equation (2.6).

On the other hand, in the GN_2 model, which has just a discrete chiral symmetry, there is no axial current conservation and $\pi(x) = 0$. Then the Eilenberger equation (2.6) again expresses the correct relation

$$\partial_\mu \langle j_5^\mu \rangle = 2\sigma(x) \langle \bar{\psi}(x)i\gamma^5\psi(x) \rangle, \quad (6.14)$$

and $\langle \bar{\psi}(x)\psi(x) \rangle$, $\sigma(x)$, and $\langle \bar{\psi}(x)i\gamma^5\psi(x) \rangle$ are all inhomogeneous.

VII. ALL-ORDERS GINZBURG-LANDAU EXPANSION

In this section we present another perspective on our solution, in order to illustrate what aspects might possibly

be extended to higher dimensional inhomogeneities. While a direct application of the resolvent approach, or the inverse scattering approach, to higher dimensions is problematic, one approach that can be straightforwardly generalized to higher dimensions consists of the Ginzburg-Landau expansion of the effective action. In this approach, one expands the free energy corresponding to the effective action (1.3) in powers of the static condensate Δ (i.e., the order parameter) and its spatial derivatives. Using the relation (2.2) between the spectral function $\rho(E)$ and the trace of the resolvent, we write the free energy density (per flavor) as

$$\mathcal{E}_{\text{free}}(x) = \frac{1}{\pi\beta} \int_{-\infty}^{\infty} dE \text{Im}[\text{tr}_D R(x; E + i\epsilon)] \times \ln(1 + e^{-\beta(E-\mu)}). \quad (7.1)$$

Thus, knowing the resolvent means we know the free energy. Usually, it is impossible to evaluate this local density of states exactly. However, an asymptotic expansion of $R(x; E)$ can always be obtained from a Laplace transform of the heat kernel expansion, leading to

$$R(x; E) = \frac{1}{2} \sum_{n=0}^{\infty} \frac{r_n(x)}{E^n}. \quad (7.2)$$

We stress that such an expansion can be derived in any dimension, not just in 1 + 1 dimensions. This is because the heat kernel expansion is known in any dimension. However, in 1 + 1 dimensions we now have the luxury of having found an exact solution. In this section we compare this exact solution with the Ginzburg-Landau expansion, and show in explicit detail how the gap equation for the inhomogeneous condensate is solved order by order in this Ginzburg-Landau expansion. The way this works is surprisingly simple and elegant, as shown below.

In 1 + 1 dimensions, including the Hartree-Fock double-counting correction, and renormalizing, leads to the standard Ginzburg-Landau expansion of the effective Lagrangian, the low order terms of which are

$$\begin{aligned} \mathcal{L}_{\text{GL}} = & \alpha_0 + \alpha_2 |\Delta|^2 + \alpha_3 \text{Im}[\Delta(\Delta')^*] \\ & + \alpha_4 [|\Delta|^4 + |\Delta'|^2] + \alpha_5 \text{Im}[(\Delta'' - 3|\Delta|^2\Delta)(\Delta')^*] \\ & + \alpha_6 [2|\Delta|^6 + 8|\Delta|^2|\Delta'|^2 + 2\text{Re}((\Delta')^2(\Delta^*)^2) \\ & + |\Delta''|^2] + \dots \end{aligned} \quad (7.3)$$

The low order terms are relatively simple, but high order terms rapidly become cumbersome. The coefficients $\alpha_n(T, \mu)$ are known functions of temperature and chemical potential. For example, in 1 + 1 dimensions [47,49]

$$\begin{aligned} \alpha_0 &= -\frac{\pi^2 T}{6} - \frac{\mu^2}{2\pi}, \\ \alpha_2 &= \frac{1}{2\pi} \left[\ln(4\pi T) + \text{Re}\psi\left(\frac{1}{2} + i\frac{\beta\mu}{2\pi}\right) \right], \\ \alpha_3 &= -\frac{1}{2^3 \pi^2 T} \text{Im}\psi^{(1)}\left(\frac{1}{2} + i\frac{\beta\mu}{2\pi}\right), \\ \alpha_4 &= -\frac{1}{2^6 \pi^3 T^2} \text{Re}\psi^{(2)}\left(\frac{1}{2} + i\frac{\beta\mu}{2\pi}\right), \\ \alpha_5 &= \frac{1}{2^8 \pi^4 3 T^3} \text{Im}\psi^{(3)}\left(\frac{1}{2} + i\frac{\beta\mu}{2\pi}\right), \\ \alpha_6 &= \frac{1}{2^{12} \pi^5 3 T^4} \text{Re}\psi^{(4)}\left(\frac{1}{2} + i\frac{\beta\mu}{2\pi}\right). \end{aligned} \quad (7.4)$$

Here $\psi^{(k)}$ denotes the k th derivative of the Euler digamma function $\psi(z) = d \ln \Gamma(z) / dz$.

In higher dimensions, an analogous Ginzburg-Landau expansion can be derived. The form of the $\alpha_n(T, \mu)$ is different, but known, and the form of the spatial terms $r_n(x)$ is different, but computable. In this section we consider how the NJL₂ model gap equation for inhomogeneous condensates looks in terms of the Ginzburg-Landau expansion. We first present a simple recursive way to generate the expansion to all orders, and then we show how the gap equation is solved order by order. A closely related expansion, the derivative (or gradient) expansion, which is an expansion just in powers of derivatives, but including all orders in powers of the condensate, is considered in [34].

A. Ginzburg-Landau expansion in 1 + 1 dimensions

The Ginzburg-Landau expansion of the effective action follows, by (2.2) and (2.8), from an asymptotic expansion (7.2) of the resolvent $R(x; E)$. The Eilenberger equation (2.6) generates such an expansion recursively. It is more convenient to define (as in [34])

$$g(x; E) \equiv R(x; E)\sigma_3. \quad (7.5)$$

In terms of g , the Eilenberger equation (2.6) reads

$$g' = iE[\sigma_3, g] - i[J, g], \quad J \equiv \begin{pmatrix} 0 & -\Delta \\ \Delta^* & 0 \end{pmatrix}. \quad (7.6)$$

We now define an asymptotic expansion for g ,

$$\begin{aligned} g(x; E) &= -\frac{i}{2} \sum_{n=0}^{\infty} \frac{g_n(x)}{E^n}, \\ g_n(x) &\equiv \begin{pmatrix} c_n(x) & -d_n(x) \\ d_n^*(x) & -c_n(x) \end{pmatrix}. \end{aligned} \quad (7.7)$$

The factor $-i$ comes from the large E expansion of $\mathcal{N}(E)$, as is already clear from the constant Δ case in (2.11), which also tells us that $g_0 = \sigma_3$. The Eilenberger equation implies the simple recursion formula for the $g_n(x)$:

$$g'_n(x) = i[\sigma_3, g_{n+1}(x)] - i[J(x), g_n(x)]. \quad (7.8)$$

The determinant condition $\det g = \frac{1}{4}$ fixes the c_n in terms of the d_n :

$$\begin{aligned} c_0 &= 1, & c_1 &= 0, & c_2 &= \frac{1}{2}|d_1|^2, & c_3 &= \frac{1}{2}(d_2 d_1^* + d_1 d_2^*), & c_4 &= -\frac{1}{8}|d_1|^4 + \frac{1}{2}|d_2|^2 + \frac{1}{2}(d_3 d_1^* + d_1 d_3^*), \\ c_5 &= -\frac{1}{4}|d_1|^2(d_2 d_1^* + d_1 d_2^*) + \frac{1}{2}(d_2 d_3^* + d_3 d_2^*) + \frac{1}{2}(d_4 d_1^* + d_1 d_4^*), \dots \end{aligned} \quad (7.9)$$

So, given $g_0 = \sigma_3$, we learn from (7.9) that $c_1 = 0$. Then the Eilenberger recursion equation (7.8) determines $d_1 = \Delta$, so that $g_1(x) = J(x)$. Next, knowing d_1 , we learn from (7.9) that $c_2 = \frac{1}{2}|\Delta|^2$, and from the Eilenberger recursion equation (7.8), we find that $d_2 = -\frac{i}{2}\Delta'$. Iterating this procedure we find

$$\begin{aligned} g_1(x) &= J(x), & g_2(x) &= \frac{1}{2} \begin{pmatrix} |\Delta|^2 & i\Delta' \\ i\Delta'^* & -|\Delta|^2 \end{pmatrix}, & g_3(x) &= -\frac{1}{4} \begin{pmatrix} i(\Delta'\Delta^* - \Delta'^*\Delta) & -(\Delta'' - 2|\Delta|^2\Delta) \\ (\Delta''^* - 2|\Delta|^2\Delta^*) & -i(\Delta'\Delta^* - \Delta'^*\Delta) \end{pmatrix}, \\ g_4(x) &= \frac{1}{8} \begin{pmatrix} 3|\Delta|^4 + 3|\Delta'|^2 - (|\Delta|^2)'' & -i(\Delta''' - 6|\Delta|^2\Delta') \\ -i(\Delta^{*''} - 6|\Delta|^2\Delta'^*) & -3|\Delta|^4 - 3|\Delta'|^2 + (|\Delta|^2)'' \end{pmatrix}, \dots \end{aligned} \quad (7.10)$$

The spectral function is expressed in terms of the trace of the resolvent:

$$\text{tr } R(x; E) = -i \sum_{n=0}^{\infty} \frac{c_n(x)}{E^n}. \quad (7.11)$$

Then the Ginzburg-Landau expansion (7.3) is obtained by inserting (7.11) into (7.1) and performing the energy integrals. Renormalization affects the first two terms, and the others follow from the integrals ($n > 2$) [50]:

$$\begin{aligned} \frac{1}{\beta\pi} \int_{-\infty}^{\infty} dE \text{Im} \left(\frac{-i}{(E + i\epsilon)^n} \right) \log(1 + e^{-\beta(E-\mu)}) \\ = \begin{cases} \frac{(-1)^{(n-2)/2} \beta^{n-2}}{(2\pi)^{n-1} (n-1)!} \text{Re} \psi^{(n-2)} \left(\frac{1}{2} + i \frac{\beta\mu}{2\pi} \right) & n \text{ even,} \\ \frac{(-1)^{(n-1)/2} \beta^{n-2}}{(2\pi)^{n-1} (n-1)!} \text{Im} \psi^{(n-2)} \left(\frac{1}{2} + i \frac{\beta\mu}{2\pi} \right) & n \text{ odd.} \end{cases} \end{aligned} \quad (7.12)$$

B. Gap equation to all orders in Ginzburg-Landau expansion

We now show how the gap equation (1.4) is solved order by order, to all orders in the Ginzburg-Landau expansion (7.12). There are two ways to see this. First, even though the $c_n(x)$ at high order n become extremely complicated combinations of powers and derivatives of Δ and Δ^* , when we evaluate $c_n(x)$ on a solution of the NLSE (2.13), they dramatically simplify and, for each n , reduce to something linear in $|\Delta(x)|^2$:

$$[c_n(x)]_{\text{NLSE}} = \beta_n |\Delta(x)|^2 + \gamma_n, \quad (7.13)$$

for some constants β_n and γ_n . For example, for $c_2(x) = |\Delta(x)|^2$ it is obvious, and for $c_3(x)$ it follows immediately from (4.21):

$$\begin{aligned} c_3(x) &= -\frac{i}{4} (\Delta'\Delta^* - \Delta'^*\Delta) \\ &= -\frac{1}{4} (b - 2E) |\Delta|^2 - \text{constant}. \end{aligned} \quad (7.14)$$

For c_4 , we note that the NLSE (2.13) implies that $(|\Delta|^2)'' = 4|\Delta|^4 + 2|\Delta'|^2 + 4(a - b^2/4 - E^2)|\Delta|^2 + \text{constant}$, so that

$$\begin{aligned} c_4(x) &\equiv \frac{3}{8} (|\Delta|^4 + |\Delta'|^2 - \frac{1}{3} (|\Delta|^2)'') \\ &= \frac{1}{8} (-|\Delta|^4 + |\Delta'|^2 - 4(a - b^2/4 - E^2) \\ &\quad \times |\Delta|^2 + \text{constant}). \end{aligned} \quad (7.15)$$

This expression is linear in $|\Delta|^2$ because we recall from (2.14) and (4.21) that $(-|\Delta|^4 + |\Delta'|^2)$ is linear in $|\Delta|^2$; this ensures that $\det R(x; E) = -\frac{1}{4}$ is satisfied, and shows that $c_4(x)$ reduces to the form in (7.13). Indeed, (7.13) holds to all orders in the Ginzburg-Landau expansion—the diagonal component of the Eilenberger equation (2.6) is the generator of this infinite sequence of relations.

Another related fact is that when we seek stationary points of the Ginzburg-Landau effective action with respect to variation of the condensate, we generate a sequence of equations for the condensate. At higher order n , these equations become more and more complicated, involving higher derivatives and nonlinearities. But, when evaluated on a solution to the NLSE, these variations take a much simpler form, for all n :

$$\frac{\delta}{\delta \Delta^*(x)} \int dx c_n(x) = \delta_n \Delta(x) + \epsilon_n \Delta'(x) \quad (7.16)$$

for some constants δ_n and ϵ_n . It is straightforward but instructive to verify this remarkable property for low orders. To all orders, this infinite sequence of identities is generated by the off-diagonal entries of the Eilenberger equation (2.6), so the off-diagonal entry of $R(x; E)$ in (2.12) explains why (7.16) holds at any order. To solve the gap equation, the parameters of the solution (i.e., the parameter θ) must be adjusted so that the coefficient of $\Delta'(x)$ vanishes, as explained in Sec. VI.

These observations may be a useful guide to seeking solutions to the gap equation in higher dimensions, where neither inverse scattering nor the resolvent approach is directly applicable for periodic condensates, but where the Ginzburg-Landau expansion approach is available.

VIII. CONCLUSIONS

To conclude, we have solved the inhomogeneous gap equation (1.4) in the NJL₂ model, to obtain a self-consistent condensate (4.12) that is crystalline in form. It is inherently complex, unlike the condensate in the discrete-chiral GN₂ model where the condensate is real. The complex crystal has a periodic amplitude, while its phase rotates through a certain angle over each period. This complex crystalline condensate contains all other previously known solutions to the gap equation as special cases. In addition to finding the exact condensate, we have presented the exact solution to the associated Bogoliubov-de Gennes equation (1.8) which gives the spectrum of fermions quantized in the presence of such a condensate. The spinor wave functions and single-particle energy spectrum are found in closed form, and we confirmed the consistency of the results by also solving the gap equation by Hartree-Fock. The key technical idea in our approach is to use the form of the gap equation to motivate an ansatz (2.12) for the Gorkov resolvent. For any condensate, the resolvent must satisfy the Eilenberger-Dikii equation (2.6), and so this reduces the problem to solving the nonlinear Schrödinger equation (2.13). Given this solution, and, in particular, the exact density of states (5.14), we are now in a position to study exactly the phase diagram of the NJL₂ model, extending the Ginzburg-Landau analysis in [1]. For example, once the free energy is minimized on our exact gap equation solution, the filling factor is then determined as a function of T and μ . This will be addressed in future work.

An important possible extension of this work would be to the massive NJL₂ model, in which a bare fermion mass is included in the original Lagrangian (1.1). This mass term explicitly breaks the continuous chiral symmetry, and approximate methods have found a rich structure in the associated phase diagram [47,51]. The resolvent approach presented here is easily extended to the massive case (yielding the real kink-antikink crystal condensate of the massive GN₂ system) only when the condensate is real. This is deeply related to the integrability properties of the classical equations of motion of these systems [52]. More work is needed to understand analytically the situation relevant for the *massive* NJL₂ system, where the condensate is complex. To date, no exact self-consistent inhomogeneous condensate solving the gap equation has been found for the massive NJL₂ model, except for simple embeddings of the real solutions [53]. Another possible extension is to study other 1 + 1-dimensional models, such as the Schwinger model [54,55].

The most interesting extension would be to try to extend some of these ideas to higher dimensions, for example for higher dimensional Gross-Neveu or Nambu–Jona-Lasinio models [56], or more ambitiously, to search for crystalline condensates in QCD or QCD models [57–61]. Here, the resolvent approach is not directly applicable, but the les-

sons from the way in which the Ginzburg-Landau expansion works (discussed in Sec. VII) may be useful. A numerical approach currently being developed [62], that does not rely on special features of 1 + 1 dimensions, is a numerical evaluation of the free energy, using the world-line Monte Carlo approach of Gies and Langfeld [63]. Other new lattice methods have been developed recently [64,65] to study four-fermion interactions, and it would be interesting to extend these to higher dimensions.

ACKNOWLEDGMENTS

We thank the DOE for support through Grant No. DE-FG02-92ER40716, and we thank Joshua Feinberg, Dominik Nickel, and Michael Thies for many helpful comments.

APPENDIX A: RESOLVENT OF A DIRAC SYSTEM, AND THE EILENBERGER EQUATION

In this appendix we summarize the derivation of the Dikii-Eilenberger equation (2.6) for the diagonal resolvent of a Dirac system. The interested reader is urged to consult also Refs. [35,36], and Appendix B of the first paper in [34]. Here we sketch the key features of the argument, for the sake of being more self-contained.

The important idea is simple. Recall that in one dimension, for a Schrödinger-like Sturm-Liouville operator, it is well known that the Green's function can be written in terms of a product of two independent solutions, normalized by their Wronskian [38]. An analogous construction exists for a one-dimensional Dirac operator [34–36]. Furthermore, in the Sturm-Liouville case, the coincident-point limit $R(x, x; E)$ satisfies a differential equation, known as the Gel'fand-Dikii equation (for an excellent review, see [6]), just by virtue of being written as a product of solutions to the original differential equation [38]. Likewise, for a Dirac system, the coincident-point limit $R(x, x; E)$ also satisfies an equation, just by virtue of being expressed in terms of solutions to the original differential equation. This equation is the Dikii-Eilenberger equation (2.6). The technical difference from the Gel'fand-Dikii equation arises because the Dirac operator is *first order in derivatives* and because it is a 2×2 *matrix operator*.

So, consider two independent spinor solutions $\psi_{1,2}$ of the BdG equation $H\psi = E\psi$ in (1.8), where H is the 2×2 matrix first-order differential operator in (1.7). Then we can write the resolvent (also a 2×2 matrix) as

$$R(x, y; E) = \begin{cases} \psi_1(x)R(y) & x < y, \\ \psi_2(x)L(y) & x > y. \end{cases} \quad (\text{A1})$$

The row-vector functions $R(y)$ and $L(y)$ are determined by demanding that $R(x, y; E)$ satisfy

$$(H - E)R(x, y; E) = \delta(x - y). \quad (\text{A2})$$

Integrating this first-order differential equation across the point $x = y$, we learn that

$$R(x, y; E) = \begin{cases} \frac{1}{iW} \psi_1(x) \psi_2^T(y) \sigma_1 & x < y, \\ \frac{1}{iW} \psi_2(x) \psi_1^T(y) \sigma_1 & x > y, \end{cases} \quad (\text{A3})$$

where the Wronskian W is the scalar function $W(\psi_1, \psi_2) = i\psi_1^T \sigma_2 \psi_2$. The coincident-point limit $x = y$ is given by an averaged limit as [see (2.7)]

$$R(x; E) = \frac{1}{2iW} (\psi_1(x) \psi_2^T(x) + \psi_2(x) \psi_1^T(x)) \sigma_1. \quad (\text{A4})$$

Now, express the BdG equation (1.8) as

$$\psi' = i \begin{pmatrix} E & -\Delta \\ \Delta^* & -E \end{pmatrix} \psi, \quad \psi'^T = i \psi^T \begin{pmatrix} E & \Delta^* \\ -\Delta & -E \end{pmatrix}. \quad (\text{A5})$$

Then, differentiating (A4) once with respect to x , using the fact that each of ψ_1 and ψ_2 satisfies the BdG equation (1.8) in the form (A5), we arrive immediately at the Dikii-Eilenberger equation (2.6). Furthermore, if we write $\psi_1 = (u_1, v_1)^T$ and $\psi_2 = (u_2, v_2)^T$, then (A4) says that

$$R(x; E) = \frac{1}{2i(u_1 v_2 - u_2 v_1)} \times \begin{pmatrix} u_1 v_2 + u_2 v_1 & 2u_1 u_2 \\ 2v_1 v_2 & u_1 v_2 + u_2 v_1 \end{pmatrix}. \quad (\text{A6})$$

Thus, the algebraic conditions (2.4) and (2.5) follow. The Hermiticity condition (2.3) is less immediately obvious, because this depends on E and W . However, it is clear from the definition of the resolvent that $R(x; E) = \langle x | 1/(H - E) | x \rangle$ is Hermitian for real E . The appropriate Hermiticity properties are studied in more detail in [34–36], and can also be seen from the result for the constant Δ case (2.11), and the $i\epsilon$ condition used to define the spectral function (2.2).

APPENDIX B: SOME USEFUL PROPERTIES OF ELLIPTIC FUNCTIONS

In this appendix we collect some basic facts and non-trivial identities for Weierstrass elliptic functions that are used repeatedly in this paper, in order to make the paper more self-contained. These functions play a special role because the self-consistent condensate $\Delta(x)$ and the spinor solutions $\psi(x)$ to the Bogoliubov-de Gennes equation are all expressed in terms of these functions. There are many good books on elliptic functions. Excellent classical references are [37,38]. We also found [39,40] to be particularly useful. Very roughly speaking, the Weierstrass elliptic functions are doubly periodic extensions of standard trigonometric functions:

$$\sin(z) \leftrightarrow \sigma(z),$$

$$\cot(z) = \frac{d}{dz} \ln \sin(z) \leftrightarrow \zeta(z) = \frac{d}{dz} \ln \sigma(z), \quad (\text{B1})$$

$$\frac{1}{\sin^2(z)} = -\frac{d}{dz} \cot(z) \leftrightarrow \mathcal{P}(z) = -\frac{d}{dz} \zeta(z).$$

The trigonometric functions have periodicity properties along the real z axis, but the Weierstrass functions are *doubly* (quasi)periodic. They are specified by the real and imaginary (half-)periods, ω_1 and ω_3 . It is standard to define also ω_2 by $\omega_1 + \omega_2 + \omega_3 = 0$. Then the Weierstrass sigma function is quasiperiodic under shifts by $2\omega_i$:

$$\sigma(z + 2\omega_i) = -e^{2\eta_i(z + \omega_i)} \sigma(z), \quad i = 1, 2, 3. \quad (\text{B2})$$

Here $\eta_i \equiv \zeta(\omega_i)$. In general, ω_1 and ω_3 define a fundamental parallelogram characterizing the doubly periodic nature of the Weierstrass functions. We choose a fundamental rectangle, with $\omega_1 = \mathbf{K}(\nu)$ and $\omega_3 = i\mathbf{K}' \equiv i\mathbf{K}(1 - \nu)$. The periods are then parametrized by the elliptic parameter ν that takes values in $[0, 1]$. At the limits $\nu = 0$ and $\nu = 1$, the Jacobi elliptic functions reduce to trigonometric and hyperbolic functions, respectively. Physically, they interpolate between kinklike solutions and sinusoidal ones.

The Weierstrass functions are then related to the Jacobi elliptic functions as follows. We define

$$\sigma_i(z) = e^{-\eta_i z} \frac{\sigma(z + \omega_i)}{\sigma(\omega_i)}, \quad (\text{B3})$$

and Jacobi's elliptic functions can be constructed from their ratios,

$$\text{sn}(z) = \frac{\sigma(z)}{\sigma_3(z)}; \quad \text{cn}(z) = \frac{\sigma_1(z)}{\sigma_3(z)}; \quad \text{dn}(z) = \frac{\sigma_2(z)}{\sigma_3(z)} \quad (\text{B4})$$

where the Jacobi functions have the elliptic parameter ν and the Weierstrass functions have periods $\omega_1 = \mathbf{K}(\nu)$ and $\omega_3 = i\mathbf{K}'(\nu)$.

Weierstrass's zeta function is defined as the logarithmic derivative of the sigma function:

$$\zeta(z) = \frac{d}{dz} \ln(\sigma(z)) = \frac{\sigma'(z)}{\sigma(z)}. \quad (\text{B5})$$

From (B2) it is clear that ζ is also quasiperiodic,

$$\zeta(z + 2\omega_i) = 2\eta_i + \zeta(z); \quad i = 1, 2, 3. \quad (\text{B6})$$

Here η_i is given by the zeta function evaluated on the periods $z = \omega_i$:

$$\zeta(\omega_i) = \eta_i. \quad (\text{B7})$$

Finally, the Weierstrass \mathcal{P} function is defined as

$$\mathcal{P}(z) = -\frac{d\zeta(z)}{dz}. \quad (\text{B8})$$

\mathcal{P} is doubly periodic, with periods $2\omega_1, 2\omega_3$:

$$\mathcal{P}(z + 2\omega_i) = \mathcal{P}(z); \quad i = 1, 2, 3. \quad (\text{B9})$$

Another important property of \mathcal{P} is that it satisfies the differential equation

$$\begin{aligned} \mathcal{P}'^2(z) &= 4\mathcal{P}^3(z) - g_2\mathcal{P}(z) - g_3 \\ &\equiv 4(\mathcal{P}(z) - e_1)(\mathcal{P}(z) - e_2)(\mathcal{P}(z) - e_3). \end{aligned} \quad (\text{B10})$$

This equation is the one (4.22) satisfied by the amplitude squared of the condensate, following from the nonlinear Schrödinger equation. The constants g_2 and g_3 in (B10) are known as the *invariants*, and they are parameters depending on the periods, and similarly for the e_i , with $e_1 + e_2 + e_3 = 0$, and $g_2 = -4(e_1e_2 + e_2e_3 + e_1e_3)$ and $g_3 = 4e_1e_2e_3$. With our choice of periods, these can be related to the Jacobi elliptic parameter ν as

$$e_1 = \frac{1}{3}(2 - \nu); \quad e_2 = \frac{1}{3}(2\nu - 1); \quad e_3 = -\frac{1}{3}(1 + \nu). \quad (\text{B11})$$

Just as the trigonometric and hyperbolic functions satisfy addition and product formulas, so too do the elliptic functions. Indeed, these elliptic identities generate all others as special cases. Here we list some of the important addition formulas for σ , ζ , and \mathcal{P} that we have used throughout the paper. References [39,40] are particularly good concerning these identities.

$$\frac{\sigma(u+v)\sigma(u-v)}{\sigma^2(u)\sigma^2(v)} = -\mathcal{P}(u) + \mathcal{P}(v), \quad (\text{B12})$$

$$\begin{aligned} &\frac{\sigma(u+v)\sigma(u-v)\sigma(2x)}{\sigma(u+x)\sigma(u-x)\sigma(v+x)\sigma(v-x)} \\ &= \zeta(u+x) - \zeta(u-x) - \zeta(v+x) + \zeta(v-x), \end{aligned} \quad (\text{B13})$$

$$[\zeta(u+v) - \zeta(u) - \zeta(v)]^2 = \mathcal{P}(u+v) + \mathcal{P}(u) + \mathcal{P}(v), \quad (\text{B14})$$

$$\zeta(u+v) - \zeta(u-v) - 2\zeta(v) = \frac{\mathcal{P}'(v)}{\mathcal{P}(v) - \mathcal{P}(u)}. \quad (\text{B15})$$

-
- [1] G. Basar and G. V. Dunne, Phys. Rev. Lett. **100**, 200404 (2008).
- [2] D. J. Gross and A. Neveu, Phys. Rev. D **10**, 3235 (1974).
- [3] R. F. Dashen, B. Hasslacher, and A. Neveu, Phys. Rev. D **12**, 2443 (1975).
- [4] S. S. Shei, Phys. Rev. D **14**, 535 (1976).
- [5] J. Feinberg and A. Zee, Phys. Rev. D **56**, 5050 (1997); in *Multiple Facets of Quantization and Supersymmetry*, edited by M. Olshanetsky *et al.* (World Scientific, Singapore, 2002).
- [6] J. Feinberg, Ann. Phys. (N.Y.) **309**, 166 (2004).
- [7] M. Thies, Phys. Rev. D **69**, 067703 (2004); J. Phys. A **39**, 12707 (2006).
- [8] V. Schon and M. Thies, Phys. Rev. D **62**, 096002 (2000); in *At the Frontier of Particle Physics*, edited by M. Shifman (World Scientific, Singapore, 2000), Vol. 3.
- [9] G. Eilenberger, Z. Phys. **214**, 195 (1968).
- [10] P. G. de Gennes, *Superconductivity of Metals and Alloys* (Addison-Wesley, Redwood City, CA, 1989).
- [11] D. K. Campbell and A. R. Bishop, Nucl. Phys. **B200**, 297 (1982).
- [12] K. Rajagopal and F. Wilczek, in *At the Frontier of Particle Physics / Handbook of QCD*, edited by M. Shifman (World Scientific, Singapore, 2001); arXiv:hep-ph/0011333.
- [13] R. Casalbuoni and G. Nardulli, Rev. Mod. Phys. **76**, 263 (2004).
- [14] S. Giorgini, L. P. Pitaevskii, and S. Stringari, arXiv:0706.3360 [Rev. Mod. Phys. (to be published)].
- [15] R. Peierls, *The Quantum Theory of Solids* (Oxford, New York, 1955).
- [16] Y. Nambu and G. Jona-Lasinio, Phys. Rev. **122**, 345 (1961); **124**, 246 (1961).
- [17] A. I. Larkin and Y. N. Ovchinnikov, Zh. Eksp. Teor. Fiz. **47**, 1136 (1964) [Sov. Phys. JETP **20**, 762 (1965)]; P. Fulde and R. A. Ferrell, Phys. Rev. **135**, A550 (1964).
- [18] P. de Forcrand and U. Wenger, Proc. Sci., LAT2006 (2006) 152.
- [19] U. Wolff, Phys. Lett. **157B**, 303 (1985).
- [20] T. F. Treml, Phys. Rev. D **39**, 679 (1989).
- [21] F. Karsch, J. B. Kogut, and H. W. Wyld, Nucl. Phys. **B280**, 289 (1987).
- [22] B. Horowitz, Phys. Rev. Lett. **46**, 742 (1981).
- [23] S. A. Brazovskii, S. A. Gordynin, and N. N. Kirova, Pis'ma Zh. Eksp. Teor. Fiz. **31**, 486 (1980) [JETP Lett. **31**, 456 (1980)]; Pis'ma Zh. Eksp. Teor. Fiz. **33**, 6 (1981) [JETP Lett. **33**, 4 (1981)]; S. A. Brazovskii, N. N. Kirova, and Matveenko, Zh. Eksp. Teor. Fiz. **86**, 743 (1984) [Sov. Phys. JETP **59**, 434 (1984)].
- [24] J. Mertsching and H. J. Fischbeck, Phys. Status Solidi B **103**, 783 (1981).
- [25] J. Bar-Sagi and C. G. Kuper, Phys. Rev. Lett. **28**, 1556 (1972).
- [26] A. I. Buzdin and V. V. Tugushev, Zh. Eksp. Teor. Fiz. **85**, 735 (1983) [Sov. Phys. JETP **58**, 428 (1983)]; A. I. Buzdin and S. V. Polonskii, Zh. Eksp. Teor. Fiz. **93**, 747 (1987) [Sov. Phys. JETP **66**, 422 (1988)].
- [27] K. Machida and H. Nakanishi, Phys. Rev. B **30**, 122 (1984).
- [28] R. Jackiw and C. Rebbi, Phys. Rev. D **13**, 3398 (1976).

- [29] J. Goldstone and F. Wilczek, Phys. Rev. Lett. **47**, 986 (1981).
- [30] A. J. Niemi and G. W. Semenoff, Phys. Rep. **135**, 99 (1986).
- [31] A. J. Heeger, S. Kivelson, J. R. Schrieffer, and W. P. Su, Rev. Mod. Phys. **60**, 781 (1988).
- [32] E. Witten, Nucl. Phys. **B145**, 110 (1978); **B149**, 285 (1979).
- [33] I. K. Affleck, Phys. Lett. **109B**, 307 (1982).
- [34] I. Kosztin, S. Kos, M. Stone, and A. J. Leggett, Phys. Rev. B **58**, 9365 (1998); S. Kos and M. Stone, Phys. Rev. B **59**, 9545 (1999).
- [35] L. A. Dickey, *Soliton Equations and Hamiltonian Systems* (World Scientific, Singapore, 1991).
- [36] D. Waxman, Ann. Phys. (N.Y.) **241**, 285 (1995).
- [37] I. Abramowitz and I. Stegun, *Handbook of Mathematical Functions* (Dover, New York, 2000).
- [38] E. T. Whittaker and G. N. Watson, *Modern Analysis* (Cambridge University Press, Cambridge, England, 1962).
- [39] N. I. Akhiezer, *Elements of the Theory of Elliptic Functions* (American Mathematical Society Translations, Providence, 1980).
- [40] D. F. Lawden, *Elliptic Functions and Applications* (Springer-Verlag, New York, 1980).
- [41] F. Wilczek, *Adiabatic Methods in Field Theory*, in TASI Lectures in Elementary Particle Physics 1984, edited by D. N. Williams (TASI Publications, Ann Arbor, 1984).
- [42] I. J. R. Aitchison and G. V. Dunne, Phys. Rev. Lett. **86**, 1690 (2001).
- [43] Note that we have made a Jacobi imaginary transformation $x \rightarrow ix$, which involves interchanging the real and imaginary periods, relative to the notation in [1], in order to be consistent with the elliptic parameter conventions of [7].
- [44] In general, when we allow for an overall shift of the energy spectrum by including an extra plane-wave phase in the condensate $\Delta(x)$, these functions can be written as $a(E) = 2E^2 - (\sum_{j=1}^4 E_j)E + \frac{1}{8}[(\sum_{j=1}^4 E_j)^2 - \sum_{i<j}^4 (E_i - E_j)^2]$, $b(E) = 2E - (\sum_{j=1}^4 E_j)$, and $\mathcal{N}(E) = 1/(4\sqrt{\prod_{j=1}^4 (E - E_j)})$.
- [45] A. O. Smirnov, Sbornik Math **186**, 1213 (1995).
- [46] K. Ohwa, Phys. Rev. D **65**, 085040 (2002).
- [47] C. Boehmer, M. Thies, and K. Urlichs, Phys. Rev. D **75**, 105017 (2007).
- [48] F. Karbstein and M. Thies, Phys. Rev. D **76**, 085009 (2007).
- [49] A. I. Buzdin and H. Kachkachi, Phys. Lett. A **225**, 341 (1997).
- [50] K. Urlichs (unpublished notes).
- [51] C. Boehmer, F. Karbstein, and M. Thies, Phys. Rev. D **77**, 125031 (2008).
- [52] A. Neveu and N. Papanicolaou, Commun. Math. Phys. **58**, 31 (1978).
- [53] J. Feinberg and S. Hillel, J. Phys. A **39**, 6341 (2006).
- [54] W. Fischler, J. B. Kogut, and L. Susskind, Phys. Rev. D **19**, 1188 (1979).
- [55] M. A. Metlitski, Phys. Rev. D **75**, 045004 (2007).
- [56] K. G. Klimenko, Z. Phys. C **37**, 457 (1988); S. Hands, A. Kocic, and J. B. Kogut, Nucl. Phys. **B390**, 355 (1993).
- [57] I. R. Klebanov, Nucl. Phys. **B262**, 133 (1985).
- [58] A. S. Goldhaber and N. S. Manton, Phys. Lett. B **198**, 231 (1987).
- [59] A. D. Jackson and J. J. M. Verbaarschot, Nucl. Phys. **A484**, 419 (1988); L. Castillejo, P. S. J. Jones, A. D. Jackson, J. J. M. Verbaarschot, and A. Jackson, Nucl. Phys. **A501**, 801 (1989).
- [60] N. S. Manton and P. M. Sutcliffe, Phys. Lett. B **342**, 196 (1995).
- [61] B. Bringoltz, J. High Energy Phys. 03 (2007) 016.
- [62] K. Langfeld, G. Dunne, H. Gies, and K. Klingmüller, Proc. Sci., LAT2007 (2007) 202; “Worldline Monte Carlo for fermion models at large N_f ” (unpublished).
- [63] H. Gies and K. Langfeld, Nucl. Phys. **B613**, 353 (2001); Int. J. Mod. Phys. A **17**, 966 (2002).
- [64] M. Limmer, C. Gattringer, and V. Hermann, Proc. Sci., LAT2007 (2007) 268.
- [65] U. Wolff, Nucl. Phys. **B789**, 258 (2008).